Seismic interpretation and depth conversion of Top Carboniferous in the Groningen field

NAM

Bart van Assema

Date March 2017

Editors Jan van Elk & Dirk Doornhof

General Introduction

Emphasis of geological modelling has traditionally been on the reservoir formations; the Rotliegend sandstone and the immediately overlying Zechstein formation (Ref. 1 and 2). However, for the prediction of ground motion and the determination of the hypocentre of an earthquake, the full rock column from the reservoir up to the surface and also down below the reservoir is important. In reports on the models used for Ground Motion Prediction this so-called overburden (rock above the reservoir) and to a lesser extent the underburden (rock below the reservoir) are discussed (Ref. 3 and 4).

Especially during the workshop on the maximum magnitude earthquake (Ref. 5 and 6), the faults in the overburden and underburden were discussed. In this report, the interface between the Rotliegend formation and the Carboniferous formation below the Rotliegend (i.e. top Carboniferous formation), is presented and discussed.

References

1. Technical Addendum to the Winningsplan Groningen 2013; Subsidence, Induced Earthquakes and Seismic Hazard Analysis in the Groningen Field, Nederlandse Aardolie Maatschappij BV (Jan van Elk and Dirk Doornhof, eds), November 2013.
2. Groningen Field Review 2015 Subsurface Dynamic Modelling Report, Burkitov, Ulan, Van Oeveren, Henk, Valvatne, Per, May 2016.
3. Development of Version 2 GMPEs for Response Spectral Accelerations and Significant Durations for Induced Earthquakes in the Groningen field, Julian J Bommer, Bernard Dost, Benjamin Edwards, Pauline P Kruiver, Piet Meijers, Michail Ntinalexis, Barbara Polidoro, Adrian Rodriguez-Marek & Peter J Stafford, October 2015
4. V4 Ground-motion Model (GMM) for Response Spectral Accelerations, Peak Ground Velocity and Significant Duration in the Groningen field, Julian Bommer, Bernard Dost, Benjamin Edwards, Pauline Kruiver, Pier Meijers, Michail Ntinalexis, Adrian Rodriguez-Marek, Elmer Ruigrok, Jesper Spetzler and Peter Stafford, Independent Consultants, Deltares and KNMI, June 2017 with Parameter files - V4 Ground-Motion Model (GMM) for Response Spectral Accelerations, Peak Ground Velocity, and Significant Durations in the Groningen Field, Supplement to V4 GMM, Julian Bommer and Peter Stafford, Independent Consultants, June 2017
5. Report on Mmax Expert Workshop, Mmax panel chairman Kevin Coppersmith, June 2016
6. Maximum magnitude from induced earthquakes in the Groningen field, Nora Dedontney et.al., Exxonmobil Upstream Research Company, July 2016

NAM

Title	**Seismic interpretation and depth conversion of Top Carboniferous in the Groningen field**		**Date**	March 2017
			Initiator	NAM
Autor(s)	**Bart van Assema**	**Editors**	Jan van Elk and Dirk Doornhof	
Organisation	NAM	**Organisation**	NAM	
Place in the Study and Data Acquisition Plan	Study Theme Geological Modelling (Structural Model) Comment: Emphasis of geological modelling has traditionally been on the reservoir formations; the Rotliegend sandstone and the immediately overlying Zechstein formation. However, for the prediction of ground motion and the determination of the hypocentre of an earthquake, the full rock column from the reservoir up to the surface and also down below the reservoir is important. In reports on the models used for Ground Motion Prediction this so-called overburden (rock above the reservoir) and to a lesser extent the underburden (rock below the reservoir) are discussed. Especially during the workshop on the maximum magnitude earthquake (Ref. 5 and 6), the faults in the overburden and underburden were discussed. In this report, the interface between the Rotliegend formation and the Carboniferous formation below the Rotliegend (i.e. top Carboniferous formation), is presented and discussed.			
Directliy linked research	(1) Ground Motion Prediction (2) Maximum Magnitude of Earthquakes			
Used data	Active 3D seismic data Groningen field.			
Associated organisation	NAM			
Assurance	Internal NAM			

NAM

Nederlandse Aardolie Maatschappij B.V.

Shell UPO

Seismic interpretation and depth conversion of Top Carboniferous in the Groningen field, northeast Netherlands

Date: June-2017

Issued by: Bart van Assema NAM-UPO/T/DL

EP number: EP201706201191

Name	Ref. Indicator	Role	Date	Signature
Clemens Visser	NAM-UPO/T/DGR	PG Team lead Groningen	25/7	
Jose Solano Viota	NAM-UPO/T/DGR	PG Groningen	31/7	
Remco Romijn	NAM-UPO/T/DGR	GP Team lead Groningen	25/7	

Executive summary

Until recently, the LSS_1_B depth surface was used as base reservoir depth horizon in the Groningen field static model and it was derived from an isochore map, based on top_Carboniferous well-markers. Newly processed seismic data, with improved imaging of the Saalian Unconformity lead to a seismic interpretation study of the Top_Carboniferous, which is equivalent to base reservoir. Interpretation was done in the time domain and was followed by depth conversion using a calculated reservoir velocity map. The new top Carboniferous horizon (DC_T) serves multiple purposes. It leads to better defined bulk rock volumes of the Slochteren and Carboniferous reservoir intervals and helps to calculate the GIIP volumes more accurately. Carboniferous gas volumes above the gas-water contact of the Groningen field may affect the dynamic behavior of the Rotliegend reservoir when there is pressure communication. Furthermore, the top_Carboniferous map will serve to constrain porosity trend maps from an ongoing seismic inversion study.

Seismic data quality varies throughout the field. It is negatively impacted by salt pillows and diapirs in the overburden. DC_T visibility is better in areas with a high angular unconformity. Many synthetic well logs show negative amplitudes corresponding with DC_T well markers. The largest negative amplitudes are found in the central part of the Groningen field, allowing easy picking of the Saalian Unconformity, using guided auto-track picking tool. Lower amplitudes are often diffuse and/or discontinuous and are most abundant in the northern and southern periphery. The DC_T is picked on a zero-crossing in the South, where the reservoir is relatively thin and where amplitudes become diffuse. No gas water contact (i.e. flat spot) was observed on seismic within the Carboniferous succession.

When comparing both base_reservoir surfaces, the difference between the existing LSS_1_B and newly obtained DC_T depth horizons is generally less than 10 meters for most of the Groningen field. The largest differences in depth are encountered in the Lauwerszee Trough to the West and northwest, away from well control and where poor seismic data quality is abundant. Within the Groningen field, the Carboniferous reaches above the gas-water contact, making a gas footprint of 308 km^2, which is 12 km^2 (+4%) larger compared to the footprint constrained by the LSS_1_B depth horizon.

The derived reservoir thickness map supports the current geological concept of gradual thickness increase towards the north and northwest. The only exception is a relatively thin NW-SE oriented graben, which could be due to a mispick, a wrong depth conversion or active faulting during reservoir sand deposition.

The velocity map is calculated, based on average reservoir velocities at 79 well locations and is used to convert the time thickness map to true vertical thickness. There is no obvious lateral velocity trend detected on first sight, but there is probably a subtle correlation between increasing reservoir thickness and decreasing reservoir velocities.

The Upper Rotliegend gas-bearing bulk rock volume of the current model is 145.2 bcm, which is 1.82 bcm more than the bulk rock volume constrained by the newly derived base case DC_T depth surface, meaning a decrease of -1.25%.

With a base case gas-bearing bulk rock volume of 31.0 bcm (billion cubic meters), the DC_T depth horizon defines a 6.23% larger bulk rock volume in the Carboniferous section, compared to 29.14 bcm bulk rock volume constrained by the base case LSS_1_B depth horizon. These volumes lie between gross rock volumes of 22.1 bcm and 33.5 bcm, as is quoted in older studies from the ‘70s and ‘80s, respectively.

Contents

1 Introduction

To date, static models of the Groningen field included a base reservoir depth horizon derived from an isochore map based on stratigraphic picks from wireline logs. Attempts were made to map a Top_Carboniferous surface from seismic and use that as a base_reservoir horizon. This did not lead to a satisfactory result because of the varying quality of the seismic data in the model area, and because of the variable seismic expression of the Saalian Unconformity. Recently, a newly processed seismic dataset was delivered with improved imaging of the sub_Zechstein sequence. This triggered a new attempt to map the Permo-Carboniferous boundary. This document presents the results of this effort. First, the mapping of the Top_Carboniferous in the time domain is described. This is followed by a description of the time-to-depth conversion methodologies applied to derive at a Top_Carboniferous surface in the depth domain. The latter will serve as input for subsequent static and dynamic modelling efforts.

1.1 Objectives

A better defined base_reservoir surface where seismic data steers the interpolation between well observations, serves multiple purposes. First, it leads to a better defined bulk rock volume of the reservoir interval. This helps to constrain the gas volume (GIIP, Gas Initially In Place) of the Groningen field and make a comparison with the gas volume derived from dynamic models.
Second, a refined Top_Carboniferous surface supports the assessment of gas volumes contained in areas where the Carboniferous reaches above the gas-water contact of the Groningen field. The Carboniferous gas may be in pressure communication with the overlying Rotliegend reservoir, and thus affect its dynamic behavior.
Third, the mapped Top_Carboniferous surface will serve to constrain the base of the Rotliegend reservoir in an ongoing Promise inversion study. The objective of that study is to provide porosity trend maps from seismic data. These trend maps will steer the interpolation of wireline log derived porosity between well locations.

2 Geological concept

2.1 Stratigraphy

The Silesian series of the Carboniferous form a thick stratigraphic succession throughout the Netherlands, exceeding 5500m (Buggenum & Den Hartog Jager, 2007). The top of this Carboniferous sequence in the Groningen area defines the unconformity between the Limburg Group (Carboniferous) and Upper Rotliegend Group (Permian) (figure 1-2). This unconformity is also known as the Saalian Unconformity or the Base Permian Unconformity. The Caumer and Dinkel Subgroups of the Limburg Group, shown in figure 3, subcrop the Permian deposits in the Groningen area, which is shown on the map of the northern Netherlands in figure 4. The unconformity is covered by deposits from the Upper Rotliegend Group, which consists of the interfingering Slochteren Formation (ROSL) and Silverpit Formation (ROCL). The Slochteren Formation is subdivided into the Lower and Upper Slochteren Sandstone Member (respectively ROSLL and ROSLU) and the thin Akkrum Sandstone Member ((ROSLA). These are stratigraphically separated by the Ameland Claystone Member (ROCLA) and the Ten Boer Claystone Member (ROCLT) (figure 1-2).

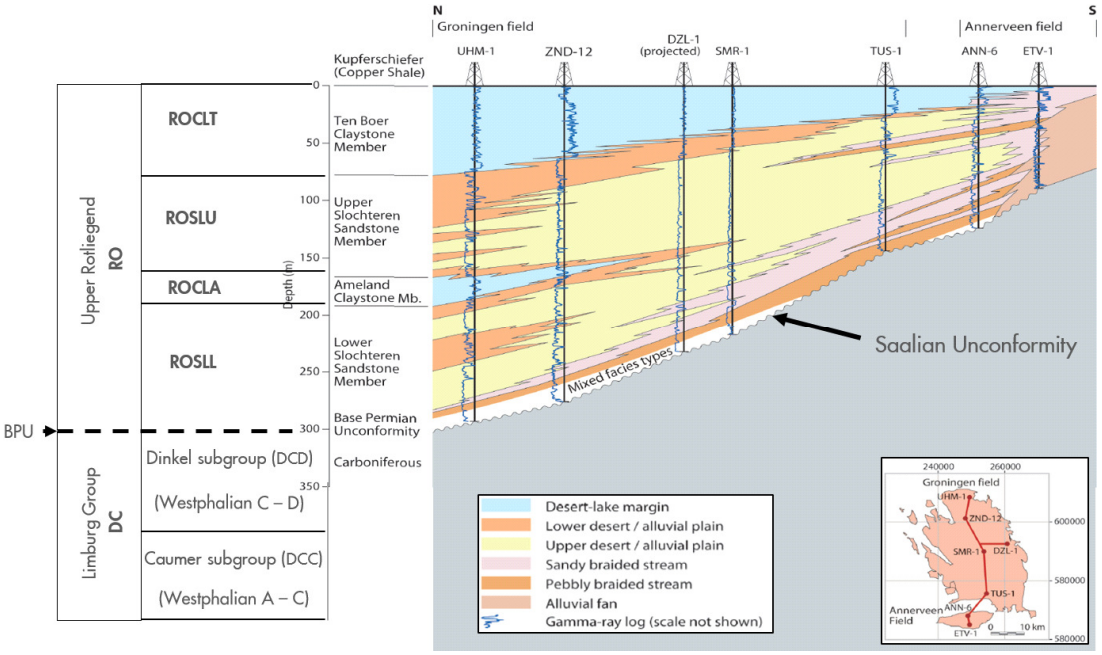

Fig. 1: Schematic cross-section of the Rotliegend facies in the Groningen field. The wells in the cross-section are indicated on the map in the lower right corner. The Carboniferous sequence is represented by the grey area in the cross-section. A general stratigraphic subdivision is shown to the left, but the Akkrum Sandstone Member is missing.

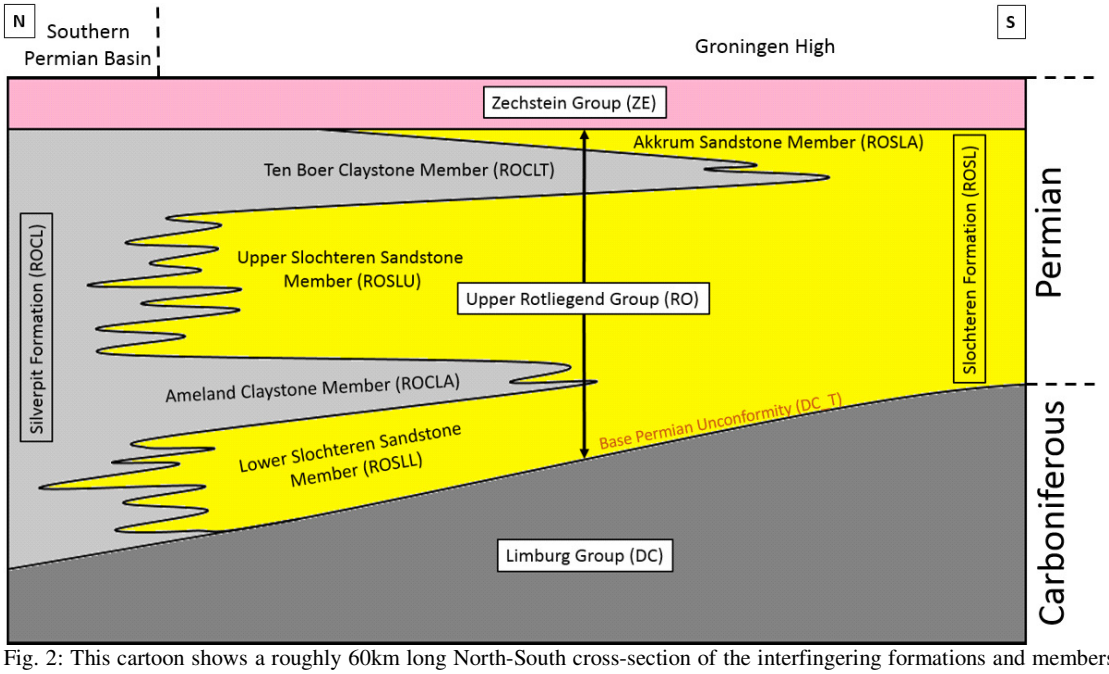

Fig. 2: This cartoon shows a roughly 60km long North-South cross-section of the interfingering formations and members of the Upper Rotliegend Group (RO) in the Groningen field at Late Permian times. Stratigraphic groups are indicated in white boxes, formations in transparent boxes, members without boxes. Sediment influx came generally from the South to southeast.

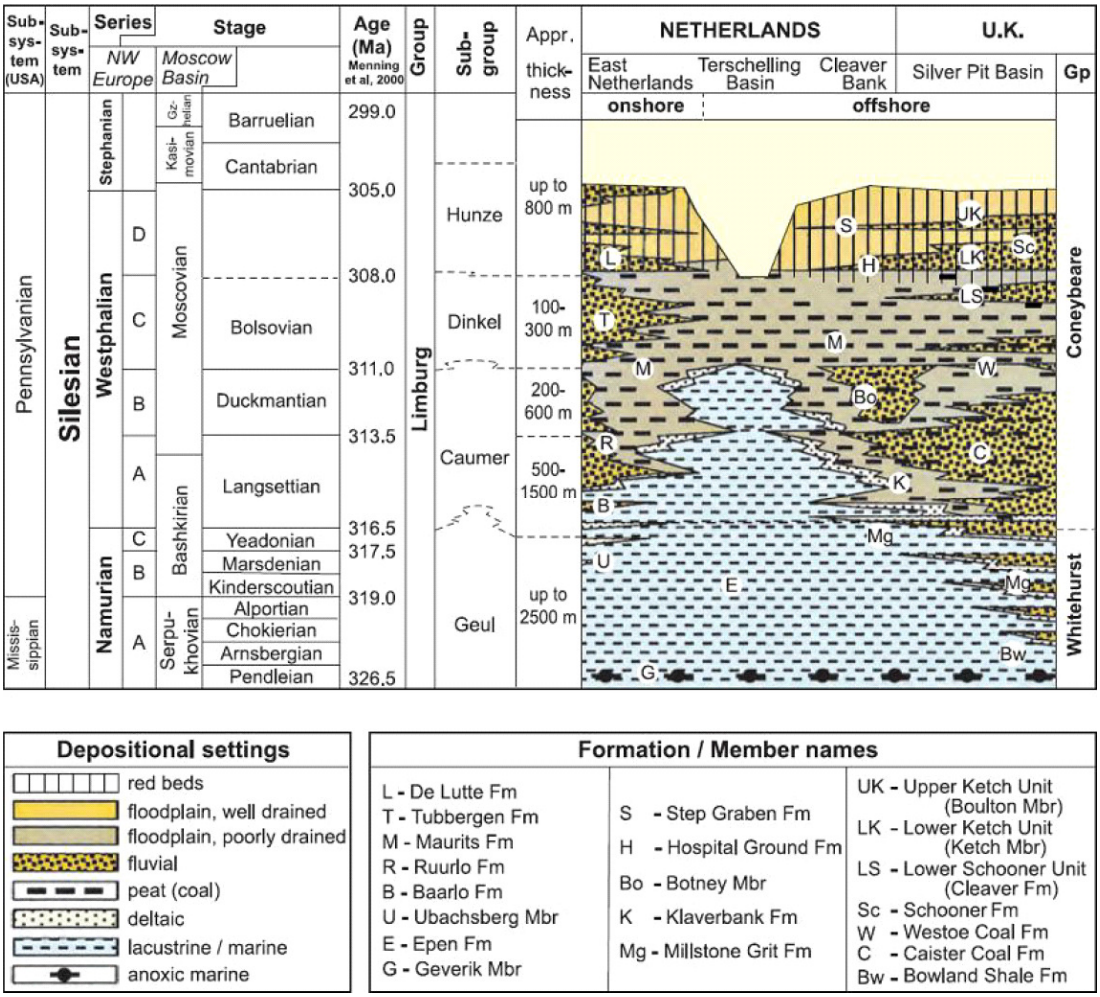

Fig. 3: Stratigraphy of the Carboniferous in the Netherlands (onshore/offshore) and United Kingdom (offshore) (Buggenum & Den Hartog Jager, 2007). The Caumer and Dinkel subgroups are the Permian subcrop in the Groningen area.

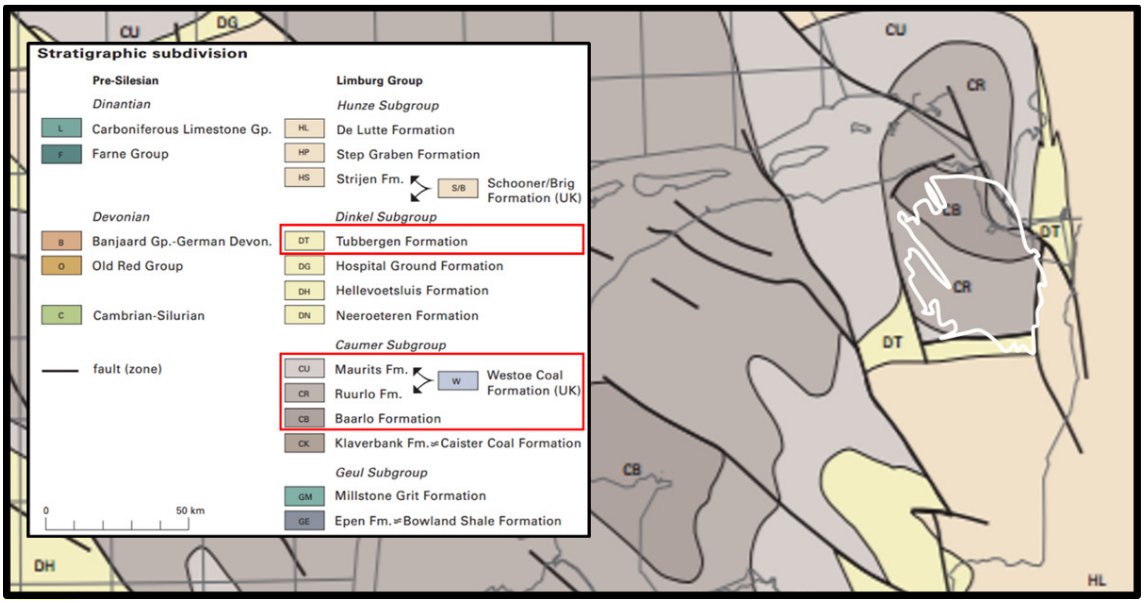

Fig. 4: Regional Carboniferous subcrop map of the northern Netherlands, onshore and offshore. The Groningen field is outlined in white, the Carboniferous formations in the study area are indicated in the red squares in the legenda (modified after https://www.dinoloket.nl/carboniferous).

Carboniferous stratigraphy – Limburg Group (DC)

Carboniferous sediments were deposited in the northern Hercynian foreland basin, which created accommodation space until the Stephanian. This was followed by Asturian inversion in the Late Carboniferous and thermal uplift in the Early Permian (Buggenum & Den Hartog-Jager, 2007). Both inversion events are expressed by the Saalian erosion event, which is a hiatus of 40-60 My. The preserved Limburg Group (DC) was deposited during the Westphalian A to Westphalian D and consists of organic sediments and fine-grained siliciclastics, which make part of a regressive megasequence (RGD-TNO Veendam-Hoogeveen, 2000). The Permian subcrop in the Groningen area consists of the Caumer and Dinkel Subgroups, which are part of this megasequence.

The *Caumer Subgroup (DCC)* consists of fine-grained, deltaic and fluvial-plain siliciclastics, intercalated with coal seams. This subgroup is subdivided in four formations: Baarlo Formation (equivalent to Early and Late Westphalian A), Ruurlo Formation (equivalent to Late Westphalian A and Early Westphalian B) and the Maurits Formation (equivalent to Late Westphalian B and Early Westphalian C). The northern equivalent of the Baarlo and Ruurlo Formation is the Klaverbank Formation (Van Adrichem Boogaert & Kouwe, 1995).

The *Dinkel Subgroup (DCD)* consists of a thick siliciclastic sequence, dominated by sandstone with intercalations of mudstone and to lesser extent coal seams. This sequence is also subdivided into four formations: Tubbergen Formation (equivalent to Early Westphalian C and Late Westphalian D), Hellevoetsluit Formation, Neeroeteren Formation and Hospital Ground Formation. Only the Tubbergen Formation is present below the Saalian unconformity in the Groningen area and it is dominated by fine- to coarse-grained sandstones, which are generally grey-white in the older deposits and pink-red in younger deposits. The Tubbergen sandstone beds vary in thickness and alternate with mudstones and few coal seams. The sandstones are mainly channel deposits of 5 to 20 meters thick with coarsening upward trends.

Middle to Upper Permian Stratigraphy - Upper Rotliegend Group (RO)

The Silverpit Formation and Slochteren Formation of the Upper Rotliegend Group were deposited under arid conditions during the Middle to Late Permian, when the Netherlands were located close to the equator on the southern margin of the East-West trending Southern Permian Basin (Ziegler, 1990; Geluk, 2007). The Permian sequence in the Groningen area has large differences in thickness, ranging from approximately 50m to the southeast to almost 400 m to the northwest.

The *Lower Slochteren Sandstone Member* (ROSLL) onlaps the deposits of the Limburg Group, is overlain by the red colored Ameland Claystone Member of the Silverpit Formation and pinches out in the southern part of the Groningen area (figure 1-2). The sandstone-dominated succession is deposited in a relatively arid climate, with no significant amount of vegetation, allowing wind and short-lived fluvial flooding events (e.g. wadi fan deposits) for the deposition of aeolian sand deposits, intercalated with conglomerates. The aeolian deposits show well-sorted parallel laminations and large-scale cross-bedding. Damp flat deposits are less well-sorted and contain argillaceous matrix (Adrichem Boogaert, 1976). The Lower Slochteren sandstones are of poorer reservoir quality than the Upper Slochteren sandstones.

The *Ameland Claystone Member* (ROCLA) is stratigraphically situated between the Lower and Upper Slochteren Sandstone Members and makes part of the Silverpit Formation, which is the overall northern equivalent of the Slochteren Sandstone members. The succession consists of red-brown colored silty- to sandy claystone, alternating with sandstone and siltstone streaks. The Ameland Claystone Member is highly variable in thickness in the Groningen area; it thickens towards the North, where the Silverpit Formation dominates, and it pinches out towards the South on the Groningen High. Within the Groningen gas field, this claystone member acts as a barrier for gas production-related upwelling of formation water. South of the pinch-out the Lower and Upper Slochteren Sandstone Members merge and become the Slochteren Formation, which has no members in that area. The southern time equivalent of the claystone is a conglomeratic sand.

The *Upper Slochteren Sandstone Member* (ROSLU) is a sandstone-dominated succession and is of better reservoir quality compared to the Lower Slochteren Sandstone Member. There are less conglomerates and more aeolian deposits, reflected by a greater proportion of well-sorted large-scale cross-bedding structures, with thin parallel laminations and very low amount of matrix. The thickness of the member is much more constant over the Groningen area compared to the Lower Slochteren

Sandstone Member, which is responsible for infill of the paleo-topography and therefore accommodates most of the onlap geometries. Towards the top of the Upper Slochteren Sandstone Member the sediments become more shaley and proceed into the Ten Boer Claystone Member (ROCLT). The top of the Slochteren Formation is defined by the top of the uppermost thick sandstone bed.

The *Ten Boer Claystone Member* (ROCLT) is situated conformably on top of the Slochteren Formation and consists of a sandy silt- and claystone succession, with intercalations of silt- and sandstone streaks. The Ten Boer Claystone Member is the southernmost extension of the Silverpit Formation and passes into the sandstone of the Slochteren Formation further southwards. Informally the member is overlain by the Akkrum Sandstone Member (ROSLA), which is a thin, white/grey colored sandstone wedge between the Ten Boer Claystone Member and the base of the Zechstein Group, and represents the uppermost part of the Slochteren Formation, which extends northward before shaling out into the Silverpit Formation.

2.2 Slochteren Reservoir Geometry

The area of the Groningen field was a topographical high during deposition of the reservoir sands. The eroded, deformed and tilted Carboniferous rocks defined the topography when deposition of the Upper Rotliegend Group started. The surrounding paleo-lows are Ems graben to the East, Lauwerszee Trough to the West and the Southern Permian Basin to the North (figure 5). The first stages of Slochteren reservoir deposition took place in paleo-lows. The infill with Upper Rotliegend sediments resulted in onlap geometries against the Base Permian Unconformity as can be seen in figure 6 and in cross-sections AA', CC' and DD' in figure 5 (Visser *et al.*, 2012). This onlap happened mainly in southward direction, away from the Southern Permian Basin center, as sedimentation of the Lower Slochteren Sandstone Member proceeded. When the Lauwerszee Trough filled up by this process, onlap of the Lower Slochteren Sandstone Member also occurred on the western flank of the Groningen High, as is studied by Berghuijs (2013) and shown in cross-section BB' in figure 5.

In summary, the current geological concept of the Slochteren formation geometry in the Groningen field includes a gradual reservoir thickening towards the center of the Southern Permian Basin to the North and Northwest. This is mainly due to the thickness increase of the Lower Slochteren Sandstone Member, since onlap occurs and is focused on the basal part of the Upper Rotliegend sequence (Berghuijs, 2013). No abrupt thickness changes due to, for example, syntectonic faults or drastic changes in paleo-topography are expected. Some Carboniferous fault sets were reactivated during later tectonic events in the Mesozoic and Cenozoic and proceeded into the overlying Slochteren formation. Picking of the Top_Carboniferous surface in areas of poor seismic data quality is guided by these concepts.

Structural Setting

Carboniferous rocks in the Groningen area are more deformed than the overlying Permian succession. NW-SE striking anticlines and synclines are found directly below the Saalian Unconformity, whereas the Upper Rotliegend deposits are not or hardly folded. Both stratigraphic systems are tilted and intensely faulted, but fault density is greater at Carboniferous level, since faulting started prior to Slochteren reservoir deposition and 90% of these faults were reactivated during the Mesozoic and Cenozoic. The boundary faults of the Groningen field initiated in the Carboniferous. During this period, first the NW-striking faults developed throughout the area, followed by N-S and (dextral) E-W striking faults. Within the Groningen field, most faults are normal faults or have an oblique strike-slip component. Faults West of the Groningen High in the Lauwerszee Trough are of post-Rotliegend age, which have accommodated dextral sense of shear. Most fault planes are dipping under high to near-vertical angle and make part of a deeper reactivated fault system, which formed by large-scale thruststacking (Vrouwe, 2013 and references therein).

Carboniferous volume estimations in Groningen field

Previous studies calculated base case Carboniferous bulk rock volumes ranging from 22.1 bcm (NAM report no. 6823, 1977) and 33.5 bcm (with respective low - / high case: 27.2 bcm / 50.4 bcm) (NAM

report no. 89.2.084, 1989). These differences resulted from different input Top-Carboniferous surfaces and GWC interpretations.

In §5.5 of this study, the bulk rock volume (GRV) of the Carboniferous is calculated at 31.0 bcm, based on the newly interpreted DC_T horizon and the gas water contact from the current model.

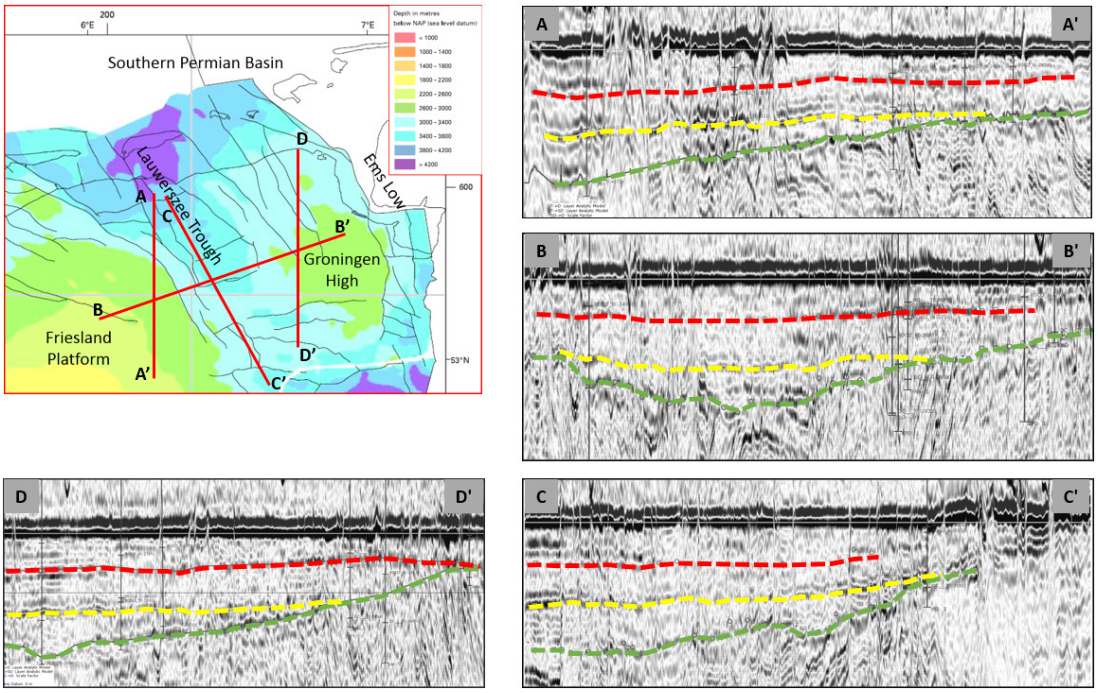

Fig. 5: General depth map of base Rotliegend in the northeastern part of the Netherlands, obtained from regional studies by TNO. Onlap structures of the Slochteren Formation are shown on seismic cross-sections in the Groningen area, as well as the Lauwerszee Trough and the Friesland Platform. Cross-section locations are indicated by the red lines on the map. Dashed lines in cross-sections: green = base Rotliegend, yellow = top Ameland Claystone Member, red = base Ten Boer Claystone Member, solid grey line = top Rotliegend (modified after Berghuijs, 2013).

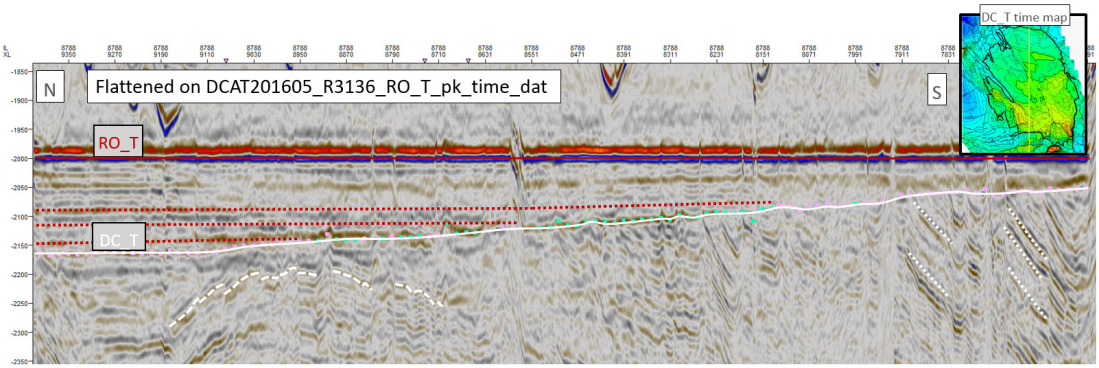

Fig. 6: Flattened N-S oriented seismic cross-section, showing faulted, tilted and folded geometries within the Carboniferous (white dashed lines) and onlap structures in the Rotliegend reservoir (red dashed lines) overlying the Base Permian Unconformity (white solid line).

3 Methodology

The base reservoir surface is made by following a workflow, which consists of two stages. The first stage covers the making of DC_T TWT (time elevation) map, and is officially approved during the

seismic interpretation review (SIR). The second stage of the workflow includes the time-to-depth conversion, the well-tie process and assessing uncertainty. The depth surface is officially approved during the DCAT (depth conversion advisory team) session.

The workflow of making a time elevation map of the base reservoir is as follows:

1. Interpretation of DC_T in seismic time cube and make seismic picking uncertainty map.
2. Calculate Rotliegend reservoir time thickness on grid lines and generate time thickness map.
3. Add time thickness map to existing interpreted Top_Rotliegend surface in time (RO_T TWT time elevation) map.

After the SIR, the workflow proceeds into the second stage in order to prepare the DC_T depth map for the DCAT session. Four different velocity models were tried for depth conversion:

- Model 1: One constant velocity in Rotliegend reservoir
- Model 2: Time thickness dependent velocities
- Model 3: Velocity map in Rotliegend reservoir, based on wells
- Model 4: Velocity map, based on inversion results

Velocities based on wells (model 3) is considered to be the most accurate option for depth conversion, because it covers lateral differences in reservoir velocity the best. Model 2 (thickness dependent velocity) was used for making the uncertainty map, since this model relates to geologic thickness trends. The next four steps in the workflow are followed:

4. Calculate Rotliegend reservoir velocity at well locations and make reservoir velocity map.
5. Calculate reservoir thickness map by multiplying the velocity map * time thickness map
6. Add reservoir thickness to RO_T (well tied) depth horizon, well-tie DC_T and make residual map.
7. Make depth uncertainty map by combining picking uncertainty and velocity uncertainty.

As the last step, after time-to-depth conversion, the GIIP volume in the Carboniferous section of the Groningen gas column is calculated:

8. Calculate Carboniferous and Upper Rotliegend bulk rock volume.

4 Seismic Interpretation

4.1 Step 1: Interpretation of DC_T in seismic time cube and make seismic picking uncertainty map

4.1.1 Seismic cube

Interpretation of DC_T is carried out in Shell Petrel 2014, on the 3D full-stack seismic time cube named "R3136_15UnrPrDMkD_Full_T_Rzn_RMO_Shp_vG". This seismic cube, covering some 2000 km^2, is latest Pre Stack Depth Migration over Groningen Field.

Seismic data quality at Carboniferous level varies significantly throughout the field. This is mainly due to salt diapirs in the overburden, but also the effect of faults and depth of the DC_T plays a major role. In general, the DC_T is better visible in areas with a high angular unconformity, but in many cases it is unclear at what seismic loop has to be picked; its exact position becomes more uncertain where a reflector either changes its polarity, its dip or when it becomes diffuse and even disappears.

Horizons used

Two horizons were used during seismic interpretation:

- Top Rotliegend → DCAT201605_R3136_RO_T_pk_time_dat
- Base Rotliegend → modeled LSS_1_B surface for comparison with own interpretation.

The LSS_1_B horizon is equivalent to Top Carboniferous (marker name: DC_T). This horizon is used in the present models and is based on an isochore, derived by LSS_1_B well-tops.

4.1.2 Picking process & picking uncertainty map

Interpretation is largely done on a seismic cube, flattened on the Top_Rotliegend surface, DCAT201605_R3136_RO_T_pk_time_dat, which makes it easier to trace the lateral thickness trend of the Rotliegend reservoir. Interpretations are checked and adjusted when necessary in the un-flattened domain. Adjustments are only needed at fault locations with anomalous reservoir thickness, due to the effects of the smooth RO_T crossing fault planes. Steps of 400m (16 increments of 25m) are between the in-lines and the cross-lines. Two areas, one in the Lauwerszee Through and one overlapping the western boundary of the field, are interpreted with 200m spacing (8 increments), due to ambiguous reflectors.

Since the DC_T reflector is mainly diffuse and not continuous throughout the field, most of the interpretation is carried out by manual picking. Guided auto-tracking is locally used in the central part of the field, where the DC_T reflector becomes more pronounced and continuous. The seismic pick uncertainty is expressed in four degrees of confidence, based on rough estimations and time sample intervals of 4ms: high confidence (±4ms), normal confidence (±8ms), low confidence (±12ms) and very low confidence (±16ms). These different areas are indicated by polygons in figure 7. The seismic interpretation is quality-checked following the SIR process.

Finally, a depth uncertainty map is calculated by combining pick uncertainty and velocity uncertainty, which can be mathematically expressed by $\sqrt{[\sigma(\text{velocity})^2 + \sigma(\text{picking})^2]} = 1\sigma$, in which σ is the standard deviation. This step is discussed in §5.4.

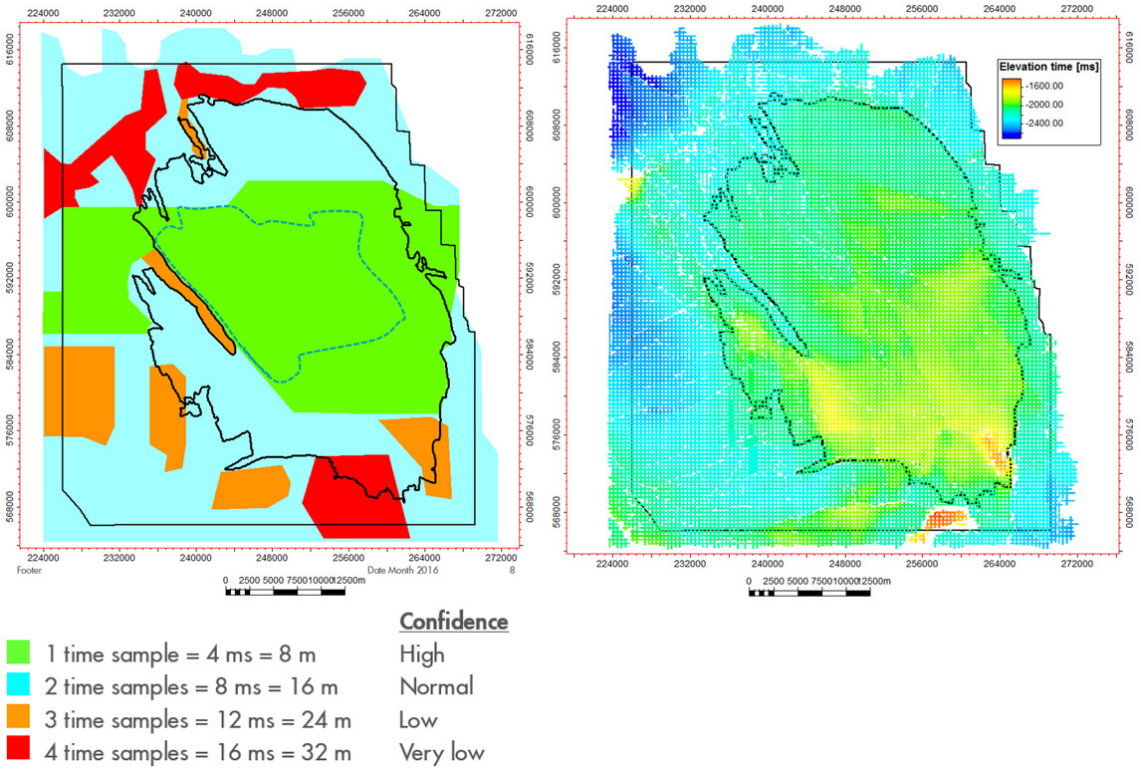

Fig. 7: Two black polygons: the outer polygon indicates the area boundary of the final depth map. The inner solid polygon is the gas footprint of the Groningen field (Rotliegend reservoir). **Left**: Colored areas indicate the seismic pick uncertainty, expressed in degree of confidence: Green = high confidence (1σ=±8m), here the area within the dashed polygon could be auto-picked; blue = normal confidence (1σ=±16m); orange = low confidence (1σ=±24m), red = very low confidence (1σ=±32m). Red areas generally indicate the location of salt diapirs. **Right**: DC_T in-lines and cross-lines in TWT domain, colored as TWT values (time elevation).

4.1.3 Synthetics

In order to establish which loop has to be picked, synthetic seismograms were made for 59 wells, spread throughout the field and its periphery (figure 8). For making synthetics, Petrel 2014 is used. Not all wells from the Groningen area can be used for making synthetics, since the majority of the wells do not penetrate the Carboniferous and do not have sonic and density logs for making synthetic seismograms. These wells are listed in Excel file "dens_sonic_data_inventory_Gron+North_combined" (\\europe.shell.com\europe\E & P\NAM Assen\Department\Onshore_Dev\Groningen Asset\Disciplines\Geology\ DC well tops & Slochteren velocities).

There are three categories for the quality of the synthetics, as shown in figure 8: high, medium and low confidence, depending on the match between reflectors of the synthetic seismic and real seismic. All synthetic images can be found in Gron_DC_T_synthetics_high_confidence.doc, Gron_DC_T_synthetics_medium_confidence.doc and Gron_DC_T_synthetics_low_confidence.doc, which are stored in the same 'DC well tops & Slochteren velocities' folder. The synthetics are created using a Ricker wavelet, with an inverted polarity, in order to have positive (blue) amplitudes from the synthetics matching with the positive RO_T reflector in the real seismic. Two examples of high confidence matches are shown in figure 9. Nine more examples for synthetics are added in Appendix A.

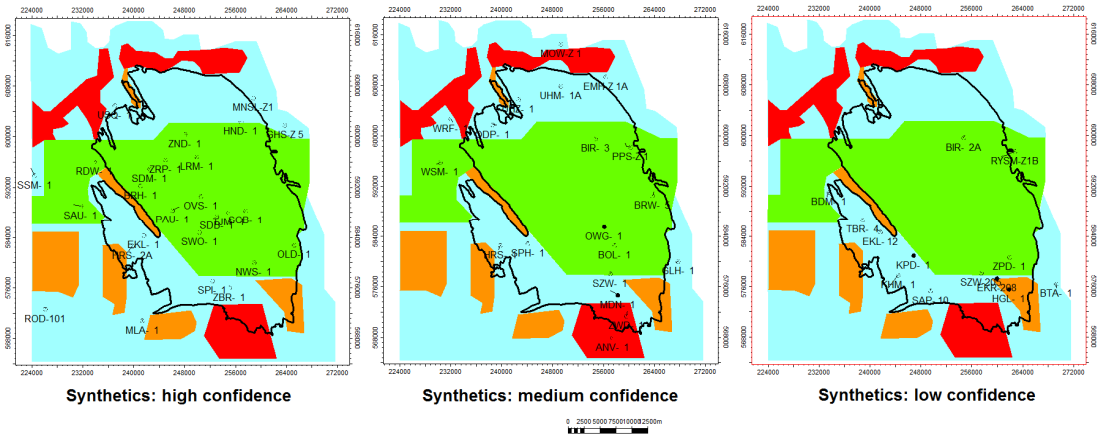

Fig. 8: Three times the same map as left image in figure 7, apart from synthetics plotted, which are categorized here in three degrees of confidence: high (27 wells), medium (19 wells) and low (13 wells) confidence. The category is depending on the quality of the match between reflectors from the synthetics and the seismic.

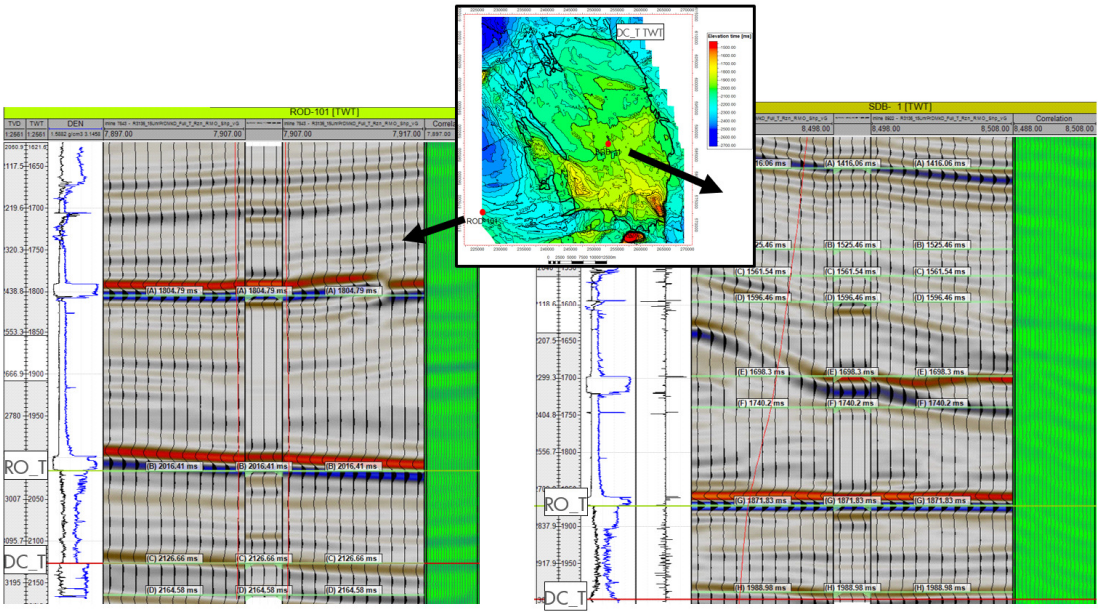

Fig. 9: Synthetic (seismic to well tie) of wells ROD-101 and SDB-1, in a normal reflectivity seismic volume. Well locations are indicated on the map. Well top DC_T in ROD-101 matches with a negative red amplitude. Well top DC_T in SDB-1 matches a zero-crossing, underneath a negative red amplitude. The majority of the DC_T well tops in the synthetics correspond to a negative red amplitude.

The synthetics often show slightly larger amplitudes than the real seismic, which might be a consequence of differences between the nature of the amplitudes in the seismic and the steps and data used for the synthetic. Matching reflectors is however still possible, since the reflector sequence is characteristic and ideally the same in both seismic and synthetic. For 33 wells (56%), the synthetics show the DC_T matches with a red, negative loop. Another 17 synthetics (29%) show DC_T matching with a zero-crossing from negative (red) to underlying positive (blue) amplitude. For three synthetics (5%) this is the other way around (zero-crossing from positive to negative) and in six synthetics (10%), the DC_T matches with a positive (blue) reflector.

Based on both the synthetics and the seismic time cube, it is concluded that in most part of the field the DC_T is characterized by a negative, red amplitude. This assumption influences choices in seismic interpretation in areas of low seismic resolution and/or ambiguous reflectors.

4.2 Step 2: Calculate Rotliegend reservoir time thickness on grid lines and generate time thickness map

The time thickness map of the reservoir, as shown in figure 10, is obtained by subtracting the DC_T time picks at the 16x16 interpretation grid from the RO_T time picks (DCAT201605_R3136_RO_T_pk_time_dat), followed by interpolation to cover the entire area. These steps are performed by the geophysicist, using the "scivision" minimum curvature gridding in nDi. This map is imported back into Petrel and converted into points, on a 25x25m grid. The Rotliegend appears to be relatively thin in the elongated, NW-SE oriented graben, in the western periphery of the field. This will be discussed in the 'Final Remarks'.

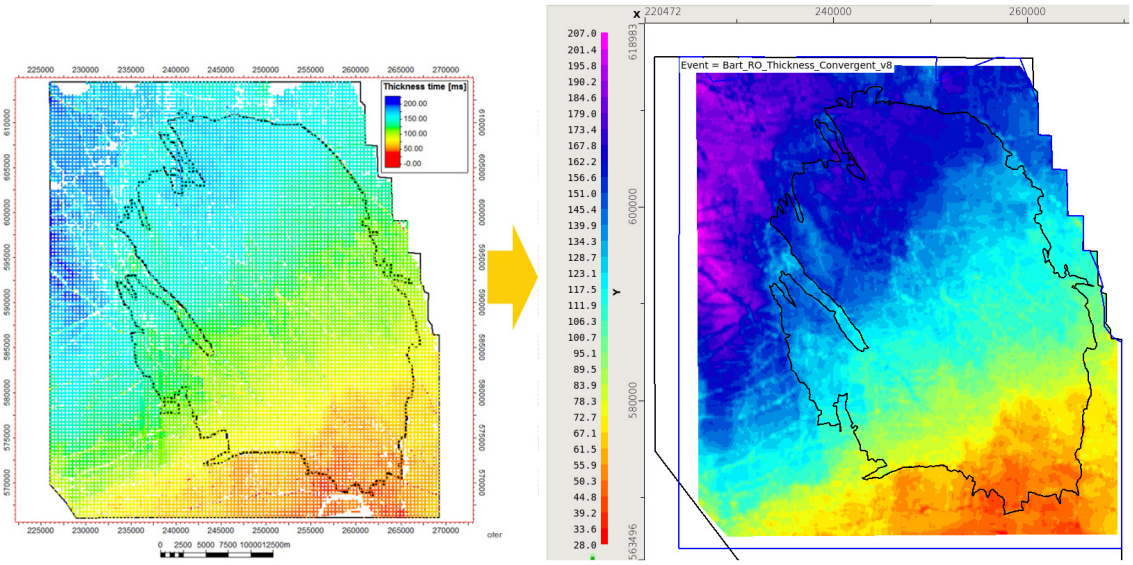

Fig. 10: **Left**: Rotliegend time thickness along in-lines and cross-lines. **Right**: Rotliegend time thickness map, interpolated in nDI. Time thickness range of 43-203 ms. Colour scheme is same for both images. Groningen field gas footprint is outlined by black polygon.

4.2.1 Final remarks on time thickness map

As was indicated in the time thickness map (figure 10) in step 2, the elongated graben in the NW periphery of the field appears to be relatively thin, compared to the area NE and SW of the graben. The constructed DC_T TWT map in figure 11 allows to check the geometry of the graben in time, showing three cross-sections through this graben. Cross-sections AA' and BB' are oriented perpendicular to the graben, showing slightly tilted fault blocks. This tilt could be an effect of the overburden salt. In the longitudinal cross section CC', the reservoir thickens gently towards the NW and shows the angular unconformity below DC_T. There is no well control and therefore the interpretation in this graben was considered to be of lower confidence. The reason for a potentially thinner Rotliegend reservoir is yet not clear. It could be due to a mispick or it has a geological reason, like syndepositional faulting. The latter is currently not supported by the geological concept, i.e. no clear indications of such a process have been found in the Groningen area at all.

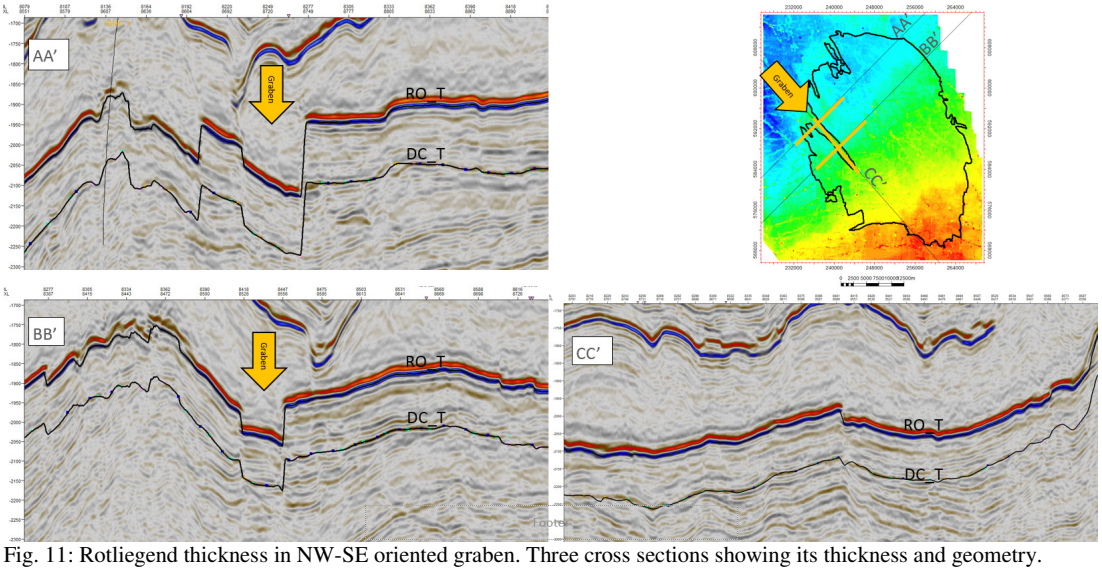

Fig. 11: Rotliegend thickness in NW-SE oriented graben. Three cross sections showing its thickness and geometry.

4.3 Step 3: Add time thickness map to existing interpreted Top_Rotliegend surface in time (RO_T TWT time elevation) map

The DC_T TWT surface in figures 12-14, is constructed by adding the Reservoir TWT thickness map to the RO_T TWT map, as is shown in the cartoon in figure 12. For this step, the time thickness map and top_reservoir map were converted to points in order to add them up in the calculator. This is followed by making a continuous TWT surface of DC_T, by 'Automatic grid size and position' and convergent interpolation algorithm in the 'Make/edit Surface' window.

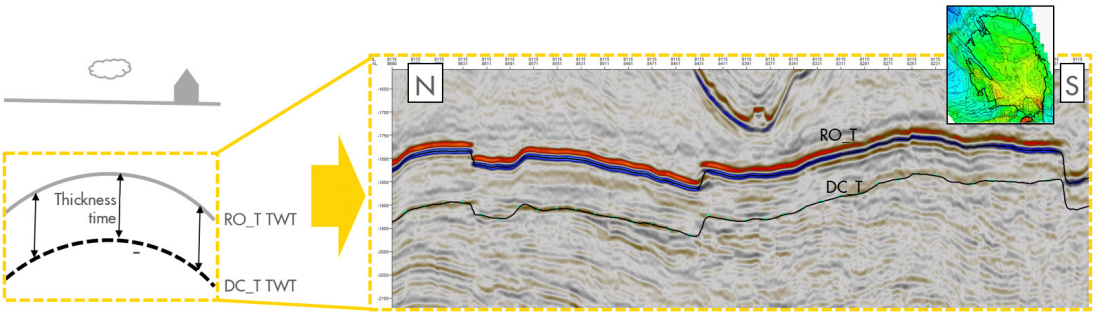

Fig. 12: **Left:** concept shown in cartoon, RO_T (TWT) + Rotliegend time thickness map = DC_T (TWT). **Right**: result in seismic time cube.

4.3.1 Resulting DC_T time map

Figure 13 shows the complete DC_T time map. Pull-up effects in the seismic time cube due to faster salt velocities are shown in figure 14, where 100ms increments of the overlying ZE_T time surface are projected on top of the DC_T time map, which is indicated in color. The same seismic picking uncertainty polygons from figure 7 are added to this figure.

An amplitude extraction map, shown in figure 15, is generated using Extract Value in the 'Surface attributes' tool. This displays the amplitude value at the seismic pick, as well as the amplitudes of the seismic on the DC_T horizon. The central part of the Groningen field shows the largest amplitudes, which corresponds to the most easily picked area, using autotrack. Lower amplitudes in the southern part of the field are due to poorer seismic data quality, higher fault density and picking of DC_T on zero-crossings in the southern periphery.

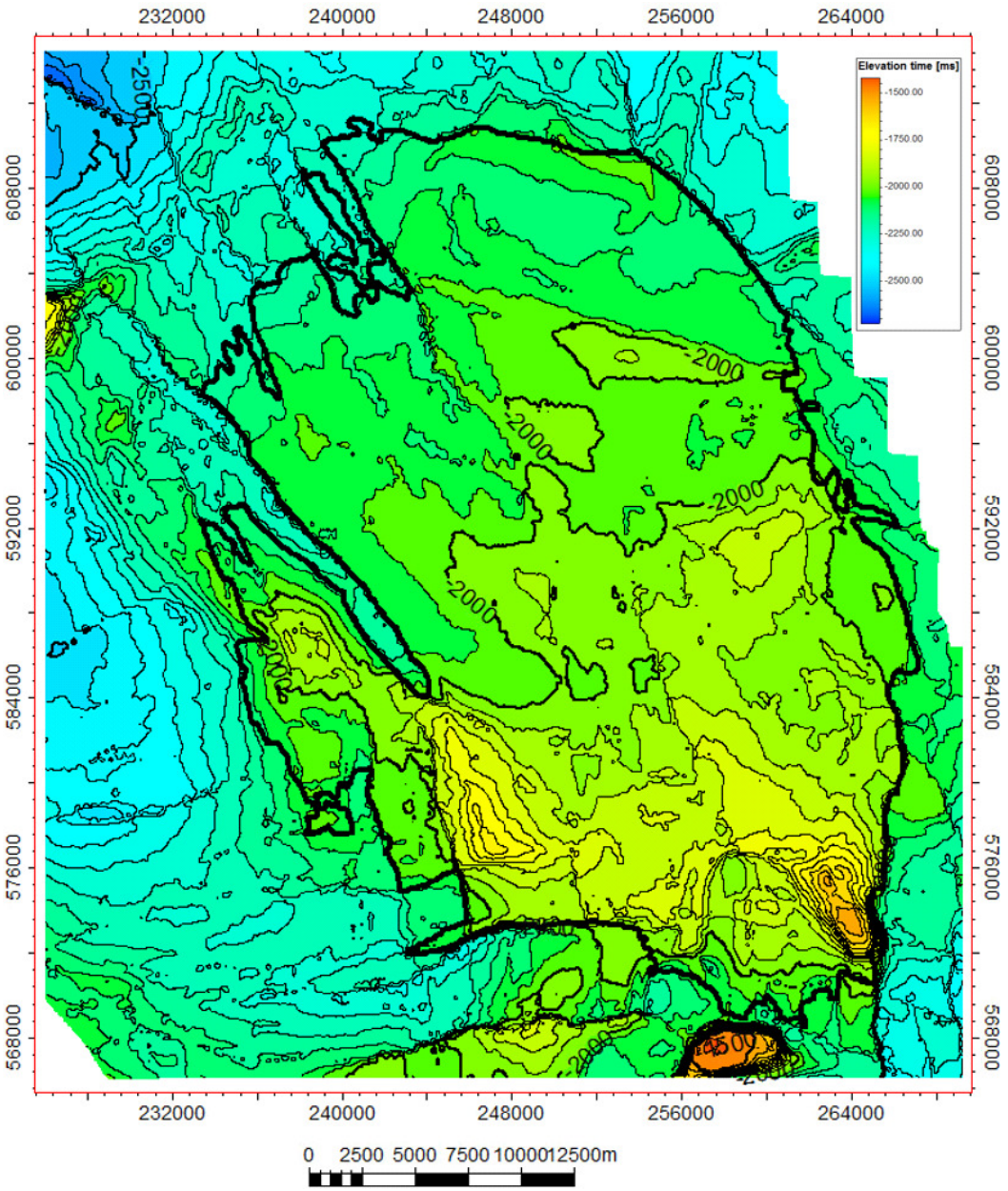

Fig. 13: Final DC_T map. High values (in red) are due to the effect of salt diapirs in the overburden. Groningen gas footprint is outlined in black polygon.

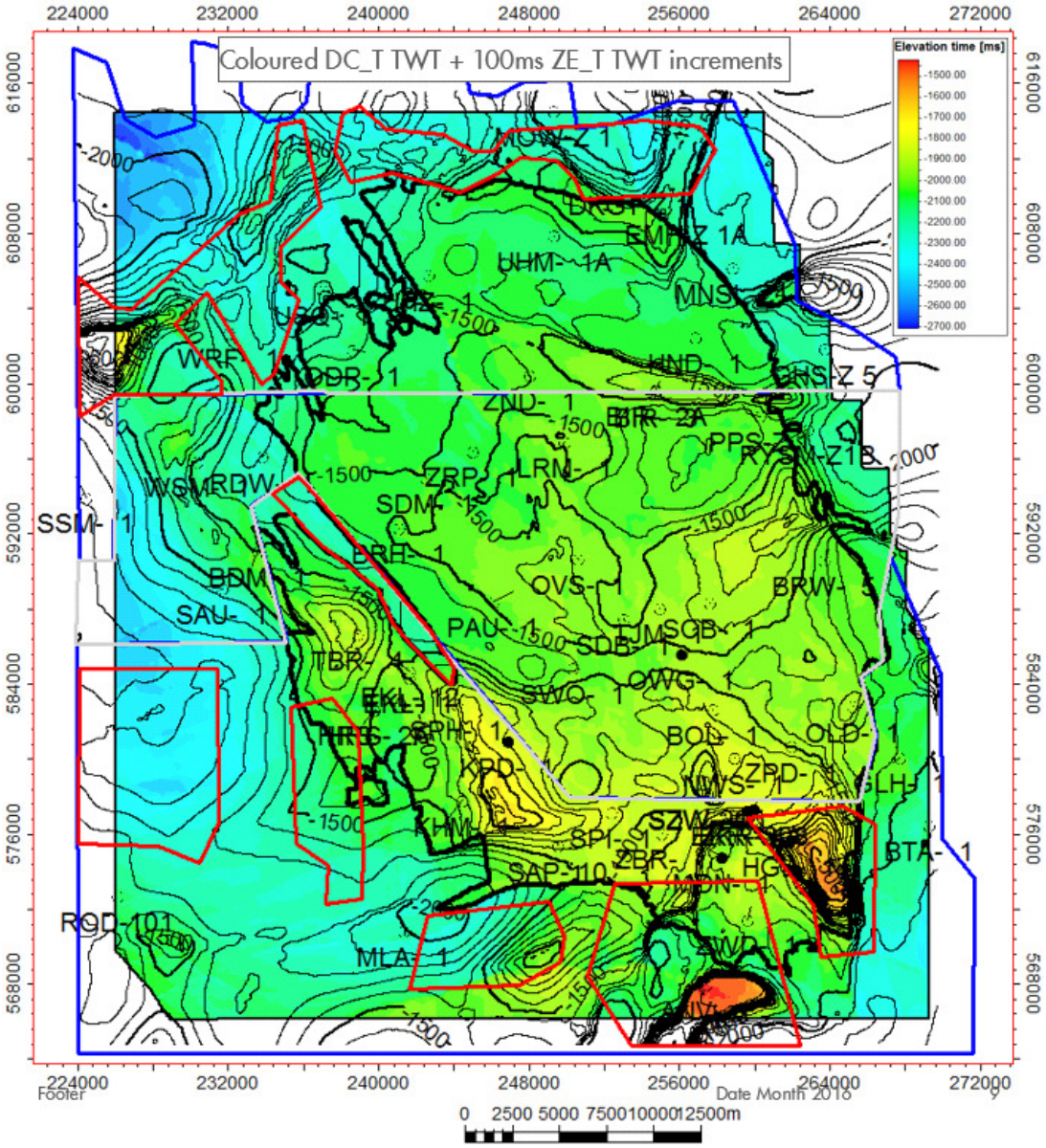

Fig. 14: Degree of confidence, projected on DC_T TWT interpretation (in color, no increments), with 100ms ZE_T line increments (no color) on top of it.

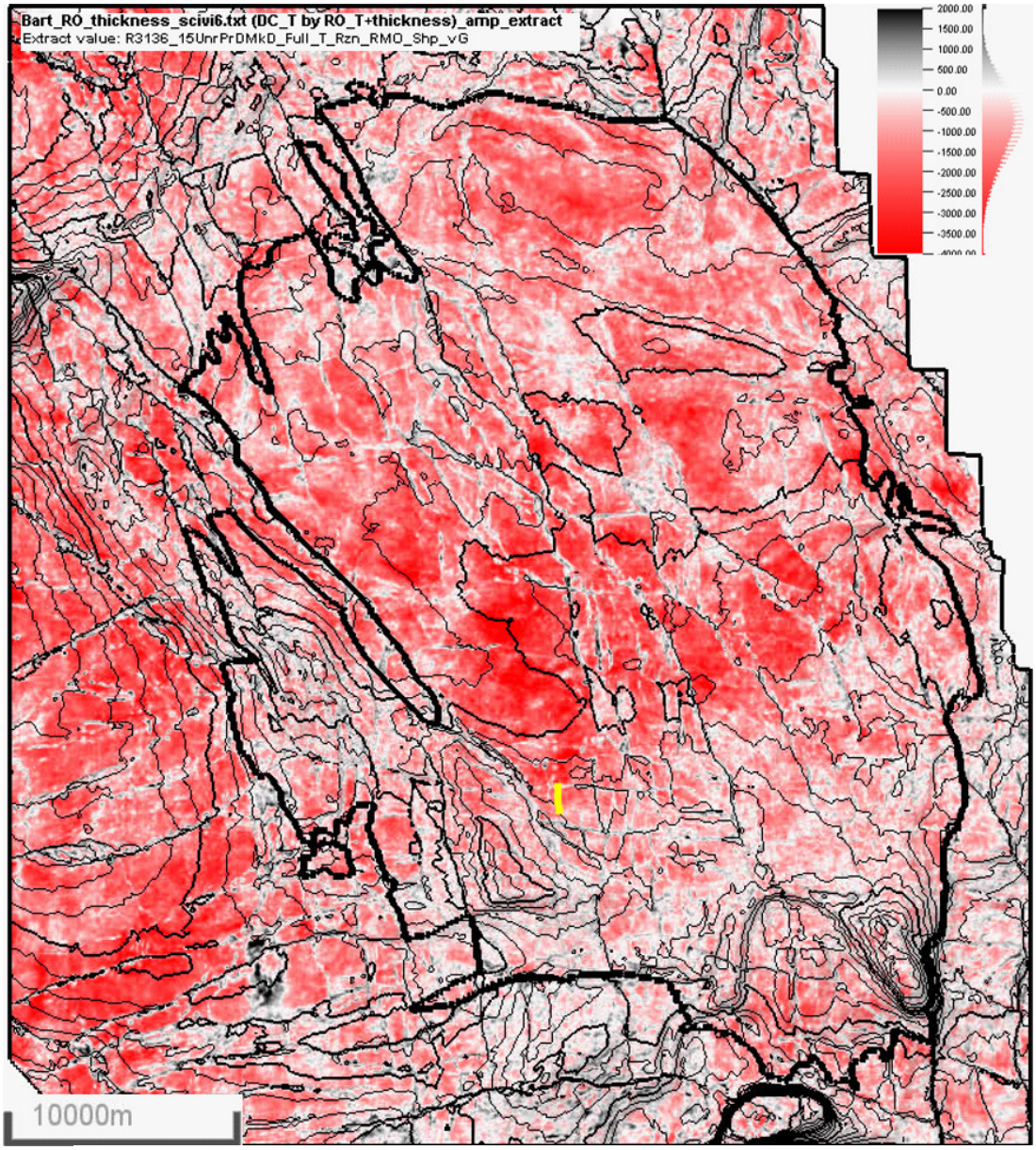

Fig. 15: Amplitude extraction map of DC_T TWT horizon, using option 'Extract Value'>search window = 0. Most part DC_T TWT surface is characterised by a red, negative amplitude.

5 Time-to-Depth Conversion

In the second stage of the DC_T seismic interpretation workflow, the time map is converted to depth, according to step 4 to 7 as described in the methodology section, followed by a rough and quick volume calculation in step 8:

4. Calculate Rotliegend reservoir velocity at well locations and make reservoir velocity map.
5. Calculate reservoir thickness map = velocity map * time thickness map.
6. Add reservoir thickness to RO_T (well tied), well-tie DC_T and make residual map.
7. Make depth uncertainty map by combining picking uncertainty and velocity uncertainty.
8. Calculate GIIP in Carboniferous section of the Groningen gas column.

5.1 Step 4: Calculate Rotliegend reservoir velocity at well locations and make reservoir velocity map

Out of the 527 available wells, 345 penetrated the DC_T depth horizon and have a usable well-marker. From these wells, the time interval and thickness interval between RO_T and DC_T were used to calculate Upper Rotliegend interval velocity at each well location. For an overview of the Slochteren velocity distribution of the 345 wells, see figure 16. Another approach is to take only one average velocity value per cluster location. Together with single well velocities, a reduced dataset of 79 velocities is obtained, which is much better suited for spatial inter/extrapolation. See table 1. A minimum curvature interpolation was used to generete the continuous interval velocity map of figure 17.

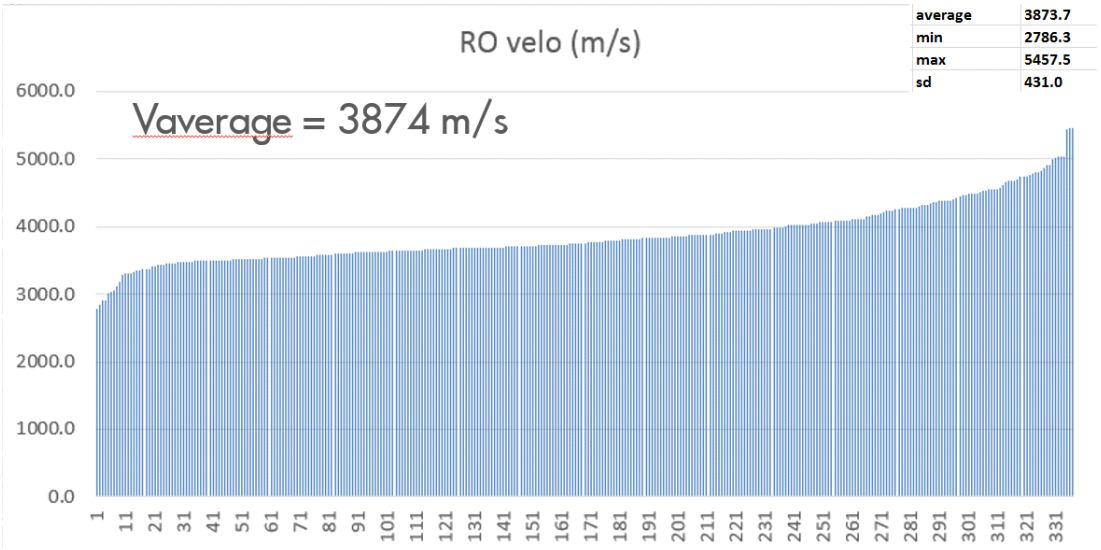

Fig. 16: An overview of the Slochteren velocity distribution from 345 wells and average velocity.

Well name	Latitude	Longitude	Velocity (m/s)
AMR-8	256433.6	591655.1	3620.7
ANN-5	248492.7	567573.4	4300.2
ANS-1	244067.4	566005.3	4832.0
ANV-3	255201.3	566546.0	4493.9
BDM-1	233252.4	590357.0	3494.9
BHM-3	266579.0	568985.0	3554.3
BIR-1	254727.4	599588.6	3677.1
BOL-1	257716.5	582606.3	3489.6
BRH-1	240995.6	592358.5	3345.9
BRW-2	263523.4	590531.7	3503.3

Well name	Latitude	Longitude	Velocity (m/s)
PAU-2	245828.7	588297.3	3733.0
POS-9	245724.9	591236.9	3620.9
PPS-Z1	259402.5	598827.7	3663.5
RDW-1	233970.3	596169.8	3845.4
ROD-101	226078.9	572698.6	3565.1
ROD-201A	226924.4	571298.3	3983.8
ROT-1A	258119.4	579628.3	3791.3
SAP-15A	248881.7	573574.9	4738.7
SAP-6	249571.4	575618.6	3987.9
SAU-1	230542.8	589276.2	3895.2

BTA-1	269321.9	575738.9	3356.6
DZL-1	260654.8	591994.9	3662.6
EKL-9	241400.3	584377.7	3491.6
EKR-201	259710.4	577259.2	4562.9
EMH-Z1A	256264.3	609325.7	3851.4
FRB-4	248121.0	578857.0	3922.6
FRM-1C	258233.3	596604.4	3823.0
GHS-Z5	263679.3	601870.6	4079.8
GLH-1	267409.5	579804.7	3662.8
HAR-1A	238120.9	576831.5	3875.3
HGL-1	261819.7	575596.8	4081.0
HGZ-1	244228.4	572346.4	4995.6
HND-1	256867.5	602469.9	3854.4
HRS-1	239514.3	581812.7	3671.6
KHM-1	243024.2	575958.9	4418.1
KPD-10A	246633.6	581138.1	3954.3
KWR-1A	247472.8	572341.4	5059.1
LRM-2	249932.5	596968.7	3530.3
MDN-1	257198.6	575376.6	4431.8
MLA-1	241391.8	570683.3	4889.9
MNSL-Z1	258788.8	606158.5	3936.0
MOW-Z1	249108.2	614503.9	4017.7
MWD-5	264261.0	578640.3	3723.2
NBR-5	255035.1	579474.2	3687.1
NWS-7	258972.8	580182.2	3979.1
ODP-1	239164.6	601702.1	3387.1
OLD-1	265263.8	582885.5	3343.5
OPK-4A	261361.6	569944.6	3817.0
OVS-8	250431.9	590794.5	3698.8
OWG-5	256109.1	585886.4	3570.1
SCB-9	257478.2	588444.4	3580.6
SDB-1	253082.1	587313.2	3833.2
SDM-1	242426.2	595138.8	3440.1
SLO-2	246323.9	579272.8	3751.3
SMR-1	253512.6	589479.7	3737.6
SPH-1	244321.8	583140.1	3866.5
SPI-8	252345.3	577171.6	3714.3
SSM-2	225943.9	593015.2	4011.0
SWO-1	250372.2	584836.8	3598.0
SZW-6	257191.8	578034.2	4393.5
TJM-10	254978.8	588193.0	3586.9
TUS-8	254355.9	575135.3	3883.1
UHM-1A	249376.0	607949.1	3536.1
UHZ-1	242629.2	605820.6	3567.8
USQ-1	237058.2	604909.0	3933.6
UTB-3	255302.1	577541.6	3568.2
VRS-2	233608.0	566335.2	4473.6
VRS-4	230421.4	569329.9	3697.4
WBL-1	245160.9	580860.2	3958.6
WDV-1	250566.4	568108.1	4072.3
WSM-1	229783.2	595586.9	3797.5
WTD-1A	253248.0	568464.7	4479.6
ZBR-1	255051.2	576012.0	3574.5
ZND-1	248045.1	600481.1	3513.2
ZPD-10	262014.6	580706.7	3527.5
ZRP-1	245007.7	596476.5	3515.9
ZVN-3	253262.5	579217.9	3720.4
ZWD-1	259781.9	572137.5	4529.7
ZWD-2A	258358.2	571002.7	4805.8

Table 1: Coordinates of 79 well locations and/or cluster locations, and corresponding reservoir velocities.

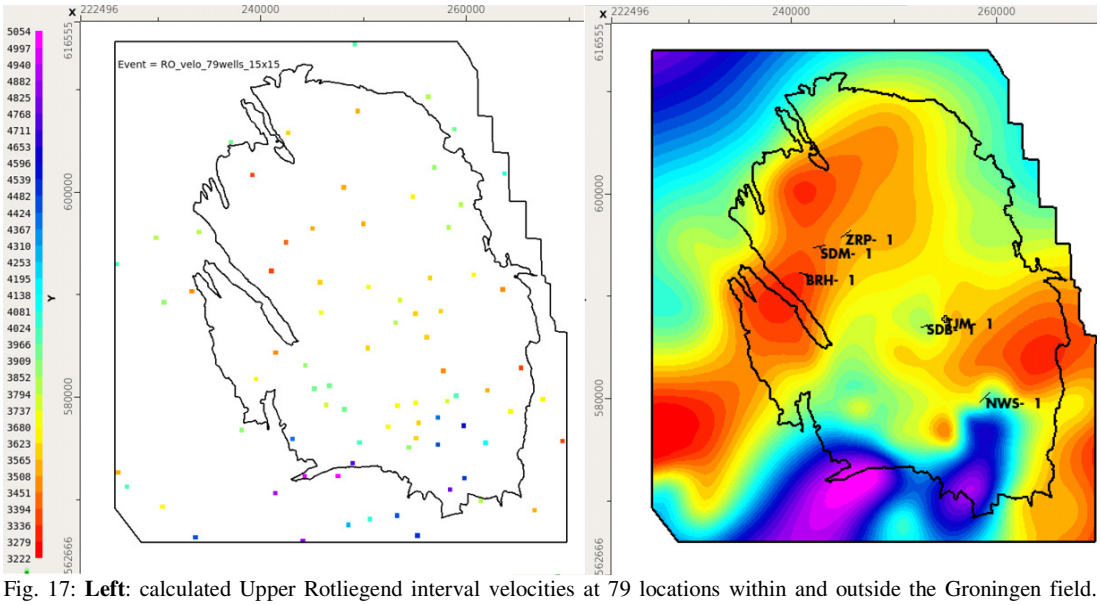

Fig. 17: **Left**: calculated Upper Rotliegend interval velocities at 79 locations within and outside the Groningen field. The locations of these velocities are either actual well locations or the averaged coordinates of multiple wells from one of the many well-clusters. **Right**: minimun curvature interpolated velocity map, derived from the reservoir velocities at well locations. The reservoir velocities of the six wells indicated on the map are compared with sonic logs in figure 18. Velocities are expressed in color from slow (red) to fast (purple).

Figure 18 shows the sonic logs of six wells at Slochteren reservoir level, combined with the average reservoir velocity at each of these well-locations, expressed in µs/ft (vertical blue lines). This qualitative observation confirms the similarity between the calculated average reservoir velocities and the estimated mean of the sonic logs. The velocities are expressed in µs/ft and the well locations are shown on the right-hand map in figure 17.

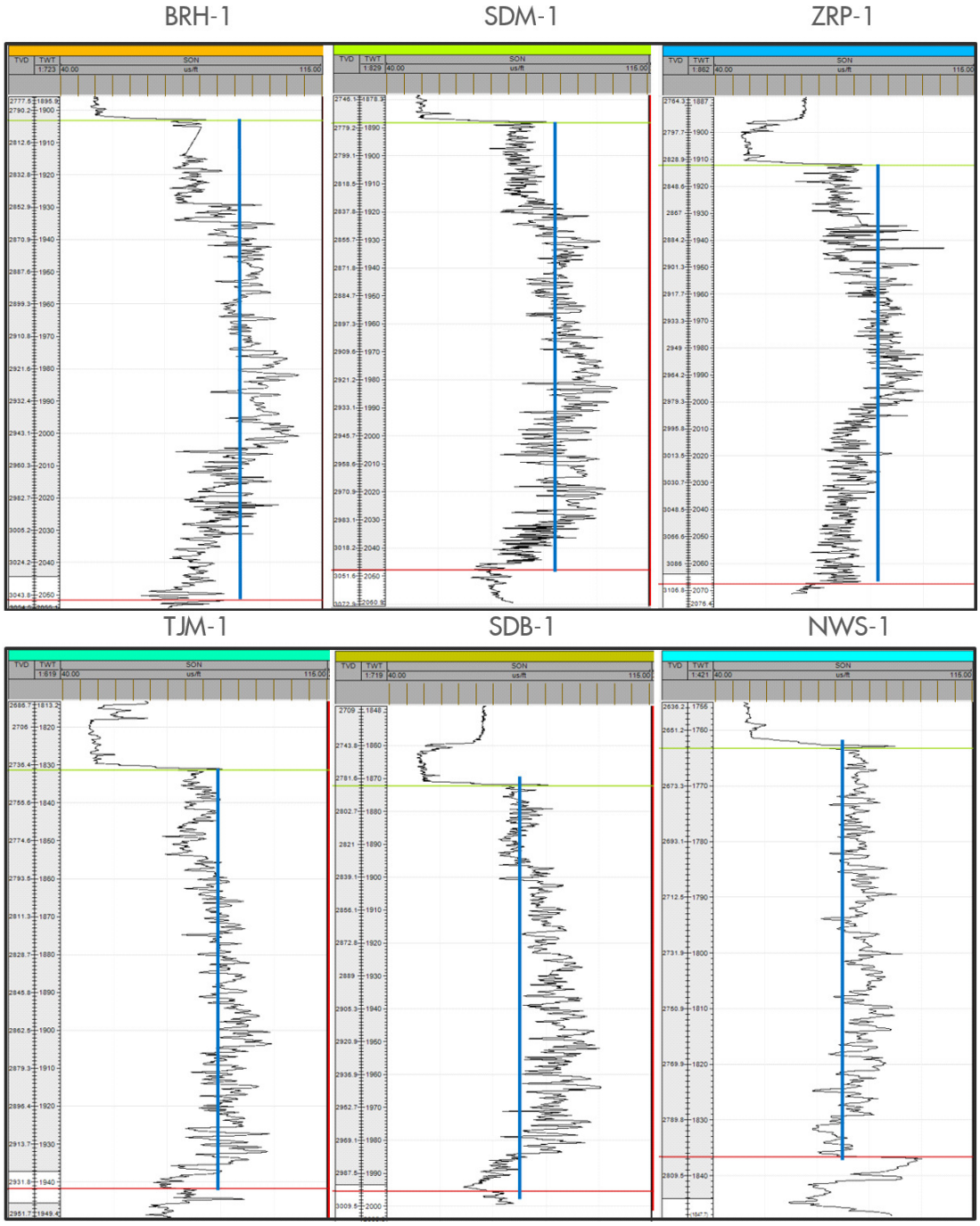

Fig. 18: Model3 velocities converted to slowness and plotted over sonic log. The brown increments on the velocity scale represent steps of 15 µs/ft. The velocity scale ranges from 40-115 µs/ft.

5.2 Step 5: Calculate reservoir thickness map by multiplying the velocity map * time thickness map

Both the time thickness map (step 2) and the velocity map (step 4) are converted to points on 25x25m grid, in order to multiply velocity by time thickness in the Petrel calculator. The outcome is a thickness grid of the Upper Rotliegend. The grid points and thickness attributes are expressed in meters and are used as input for making the convergent interpolated true vertical thickness (TVT) map. This thickness map of the Upper Rotliegend in the Groningen area is shown in figure 19. Both the Upper Slochteren gas footprint and Carboniferous gas footprint are outlined.

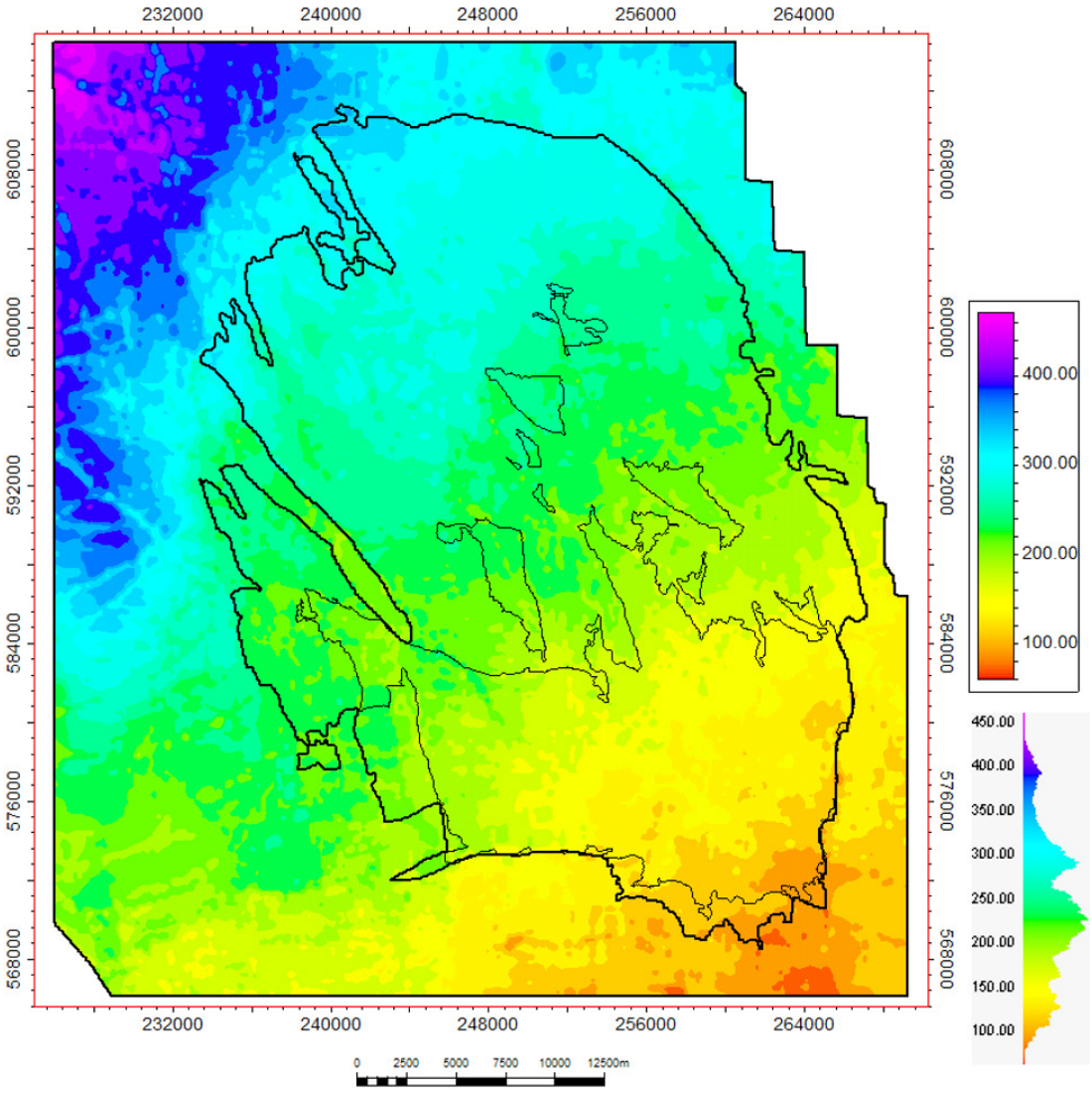

Fig. 19: thickness map (in meters) of the Upper Rotliegend in the Groningen area. Both the Slochteren (thick line) and Carboniferous gas footprint (thin line) are projected.

5.3 Step 6: Add reservoir thickness to RO_T (well tied) depth horizon, well-tie DC_T and make residual map

The thickness map of the Rotliegend reservoir is added to the well tied RO_T depth map (DCAT201605_R3136_RO_T_pk_depth_welltied.txt) to obtain the DC_T depth map. This map is subsequently tied to the wells. The wells used for this process are listed in the table in Appendix B. The residual map with colored anomaly values is shown in figure 20 and the variograms of the well-tied top and base reservoir are displayed in figure 21. The influence radius chosen is 5600m, similar to the RO_T well-ties .

The largest residuals are outside the Groningen field, except for Farmsum-1C, Eemskanaal-1 and Zuidwending-2A, which are close to the gas footprint outline (green polygon). The positive and negative extremes are +33m at Zuidwending-2A and -32m at Blijham-5C and are considered by the team geophysicist to be acceptable extremes, within the range of 1.5% of the total depth. The anomaly at ZWD-2A is at a location with poorest seismic data quality, below a salt diapir in the South of the field. This has most likely resulted in a mispick in the seismic interpretation at that location; since there is no obvious reflector, the interpretation was based on a best guess while honoring the geological concept of steady reservoir thickness increase towards the northwest. Whether there are also faults disturbing the seismic image cannot be seen. This location lies within the area of very low confidence on the seismic picking uncertainty map (see figure 7). The anomaly at BHM-5C (and -6) is also located in an area with low seismic data quality due to salt effects at the southeastern periphery, as well as the effect of a large offset fault at BHM-5C, which is shown in figure 22. The seismic picks in this area have a high uncertainty (see figure 7). The well tied depth map of top Carboniferous is shown in figure 23.

The difference map between the well-tied DC_T and the equivalent LSS_1_B from the current model is given in figure 24. Overall, the DC_T and LSS_1_B depth maps differ at max 10m for most of the Groningen field. The largest differences are to the West in the Lauwerszee Trough, where the DC_T is shallower than the LSS_1_B, and to the northwest, where the DC_T is deeper than the LSS_1_B. These areas are outside the Groningen field, but they are obvious anomalies on the map. The DC_T seismic pick has a high uncertainty in both areas and has low well-control, which adds more uncertainty to both the DC_T and LSS_1_B depth maps.

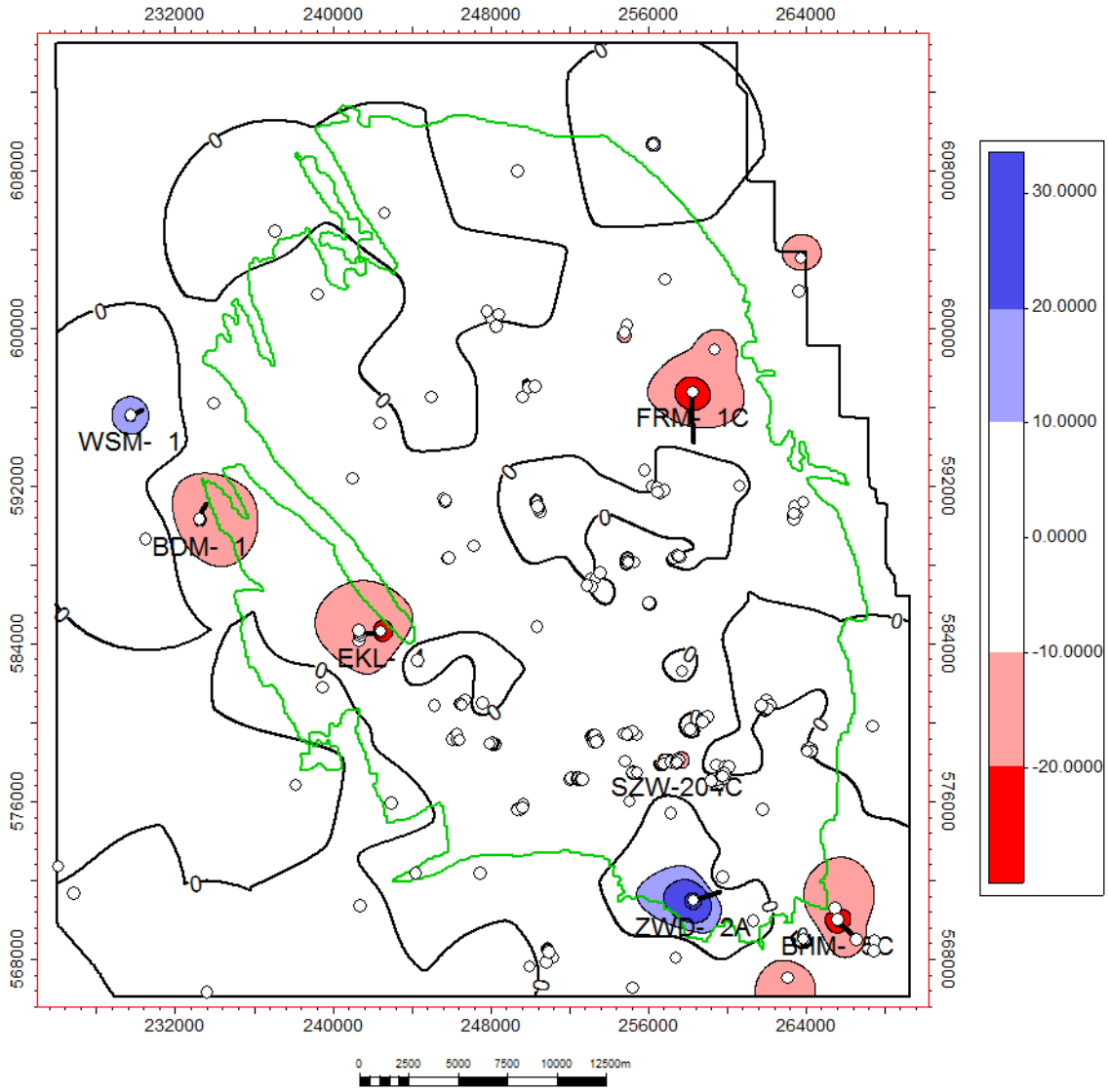

Fig. 20: Well-tie residual map of DC_T depth surface. Groningen gas footprint is outlined in green. Well-tie influence radius is 5600m. Colors change with increments every 10 meters (see also legend). White dots are well-tie locations. Well names are indicated at the six largest residuals. White dots are well-tie locations. Residual map increments every 5 meters.

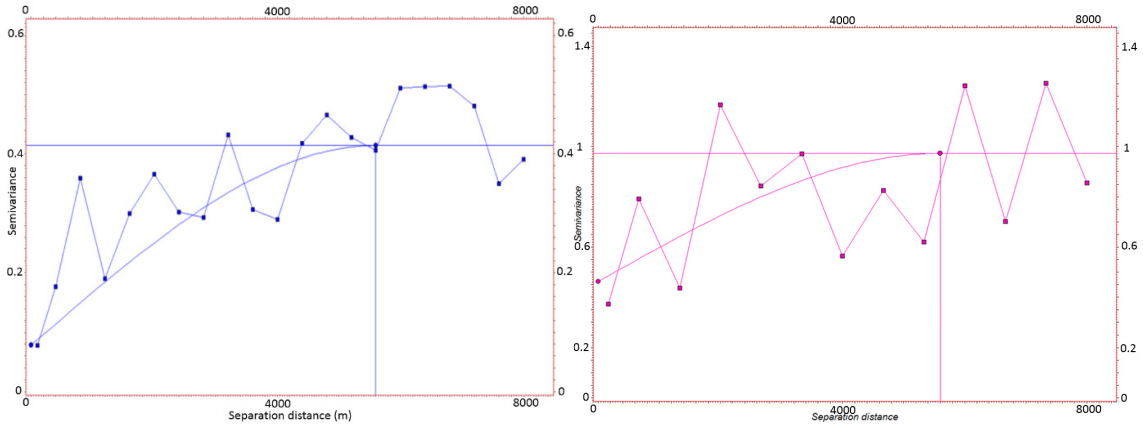

Fig. 21: **Left**: RO_T well-tie residual variogram from previous study. **Right**: DC_T well-tie residual variogram (this study). Correlation length chosen is 5600m.

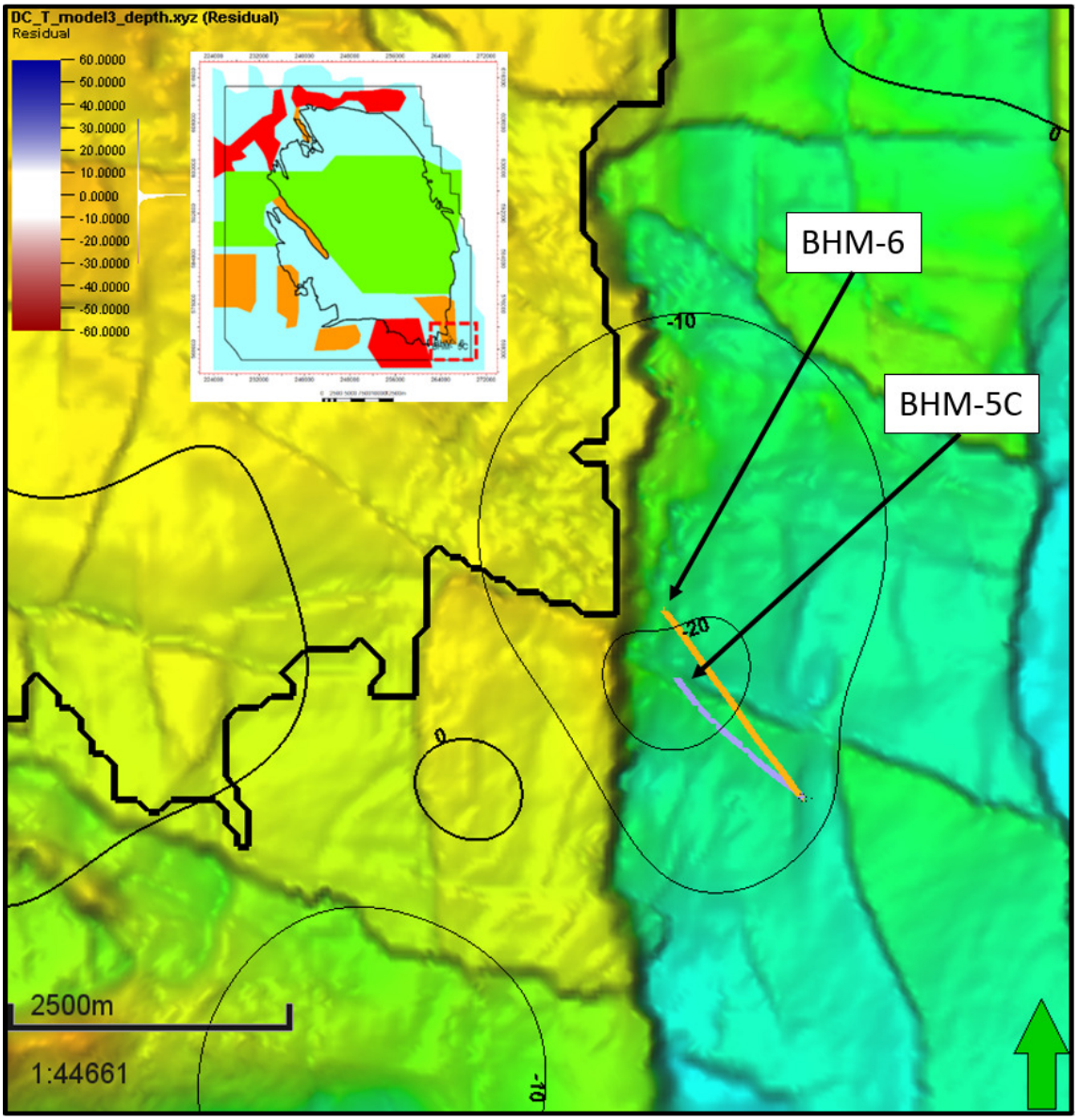

Fig. 22: BHM-5C and BHM-6 locations just southeast of the Groningen field. The residual of BHM-5C is 32m, which could be explained by salt effect of the diaper on top and/or as an effect of the fault on the seismic data quality.

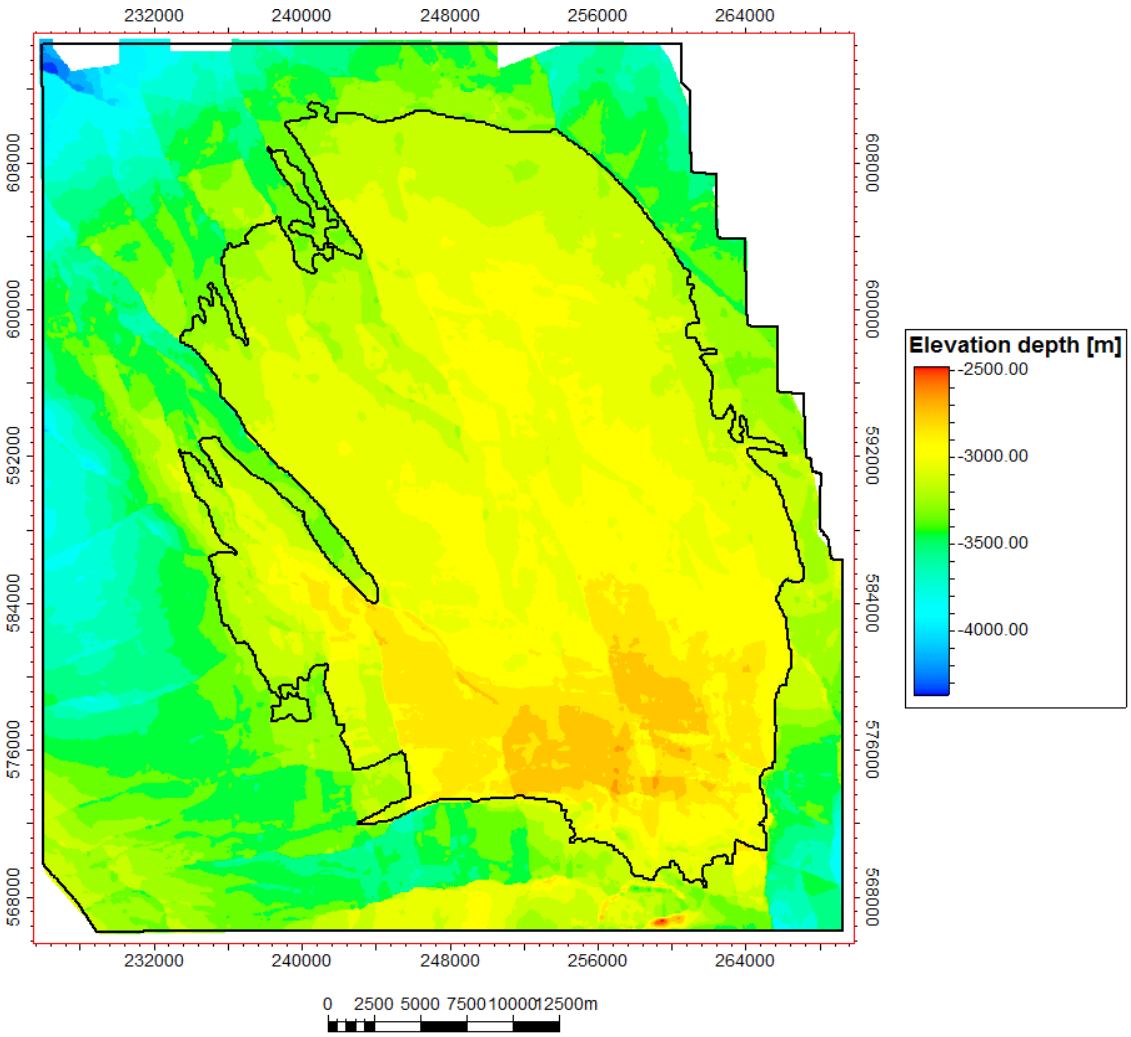

Fig. 23: Well tied DC_T depth map with depth in mTVDSS (meters True Vertical Depth sub-sea). Groningen field polygon indicated in black.

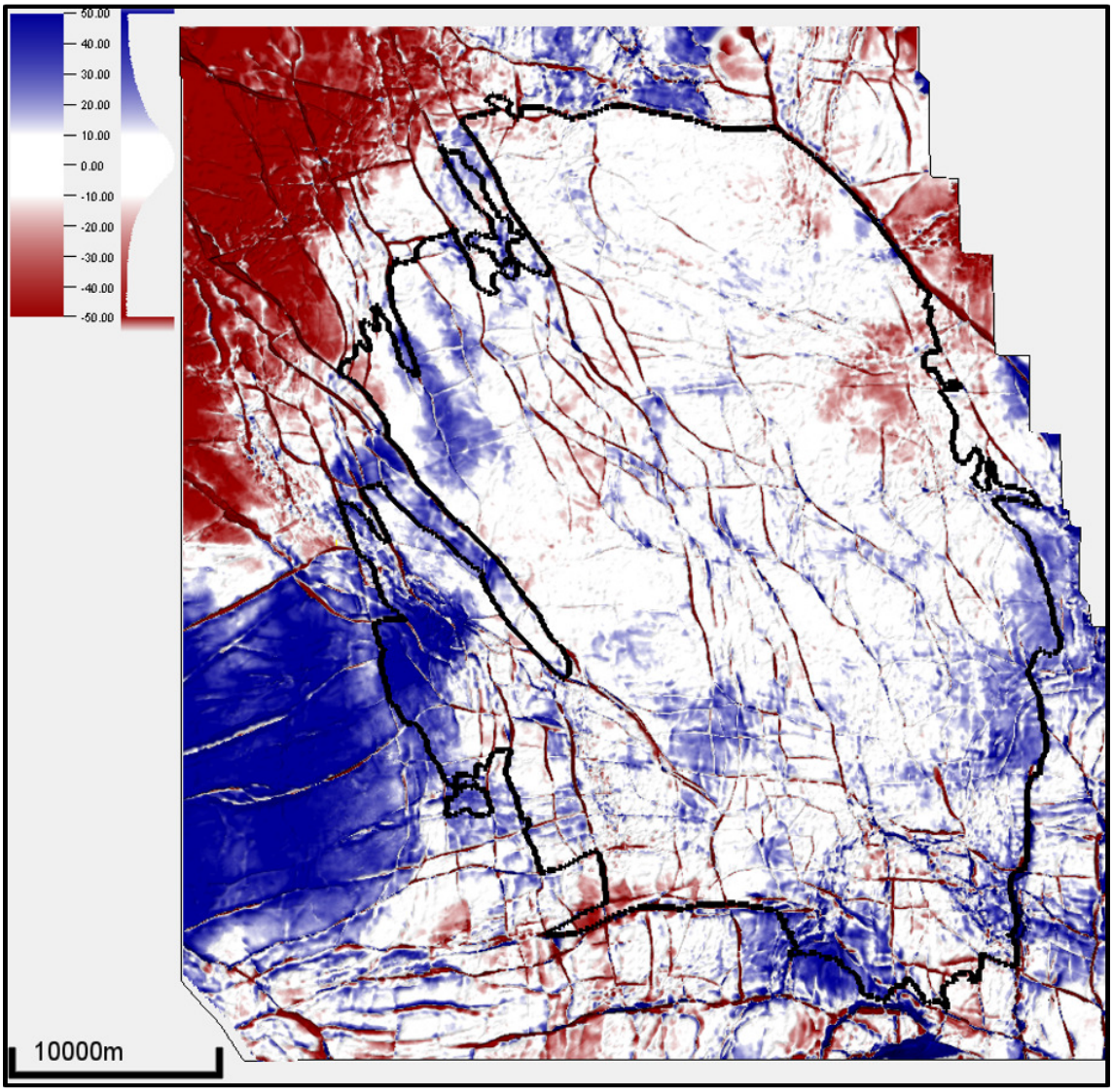

Fig. 24: The difference map between the well-tied DC_T and the equivalent LSS_1_B from the current model. In the white areas, both depth maps are less than 10m apart. Blue = DC_T depth map is shallower than LSS_1_B depth map. Red = DC_T depth map is deeper than LSS_1_B.

5.4 Step 7: Make depth uncertainty map by combining picking uncertainty and velocity uncertainty

The depth uncertainty map is derived by combining the standard deviation of the picking uncertainty map with the standard deviation of the velocity uncertainty. The first is given in figure 7 (page 12) and varies throughout the field. The latter is calculated from the residual distribution after time-to-depth conversion with velocity model 2 (see chapter 3), which relates to geological thickness trends, and is 25.8m (figure 25). The combined uncertainty is calculated by $\sqrt{[\sigma(\text{pick})^2 + \sigma(\text{velocity})^2]}$, resulting in the depth uncertainty map in figure 26. The depth uncertainty map allows to display a high case (shallow) and low case (deep) top Carboniferous depth map, apart from the base case depth map (P50) shown in figure 23. These additional scenarios are shown on the cross-sections in figures 27 and 28.

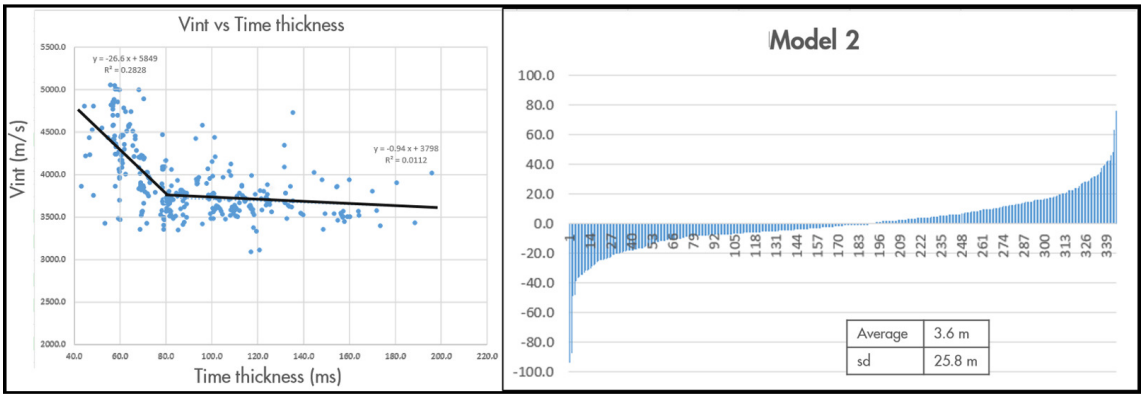

Fig. 25: **Left**: When the reservoir velocities at well locations are plotted against reservoir thickness, a general trend of increased velocity with decreased thickness can be observed. The reservoir interval velocities come from 345 wells. **Right**: DC_T well-tie residual distribution, based on velocity model 2 (thickness dependent velocities), with 1σ=25.8m.

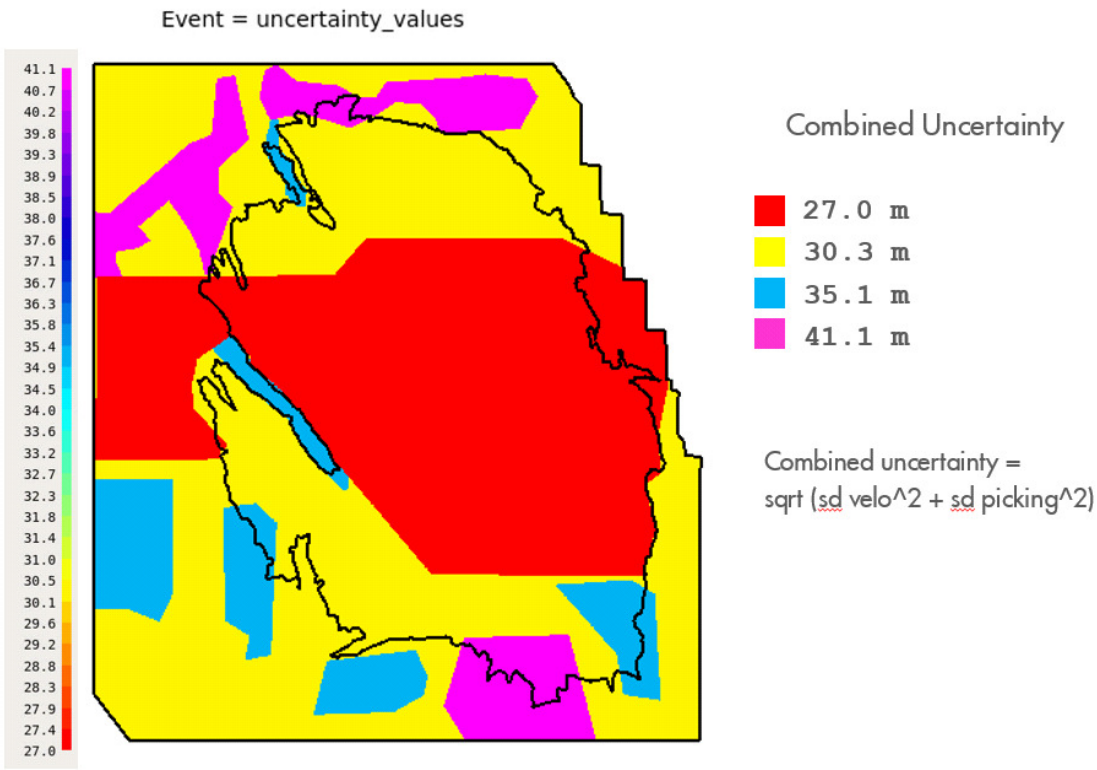

Fig. 26: Combined depth uncertainty map of the DC_T in the Groningen area, based on the standard deviations of the picking uncertainty map and velocity uncertainty. Colors represent depth uncertainty ranges, as is shown in the legend.

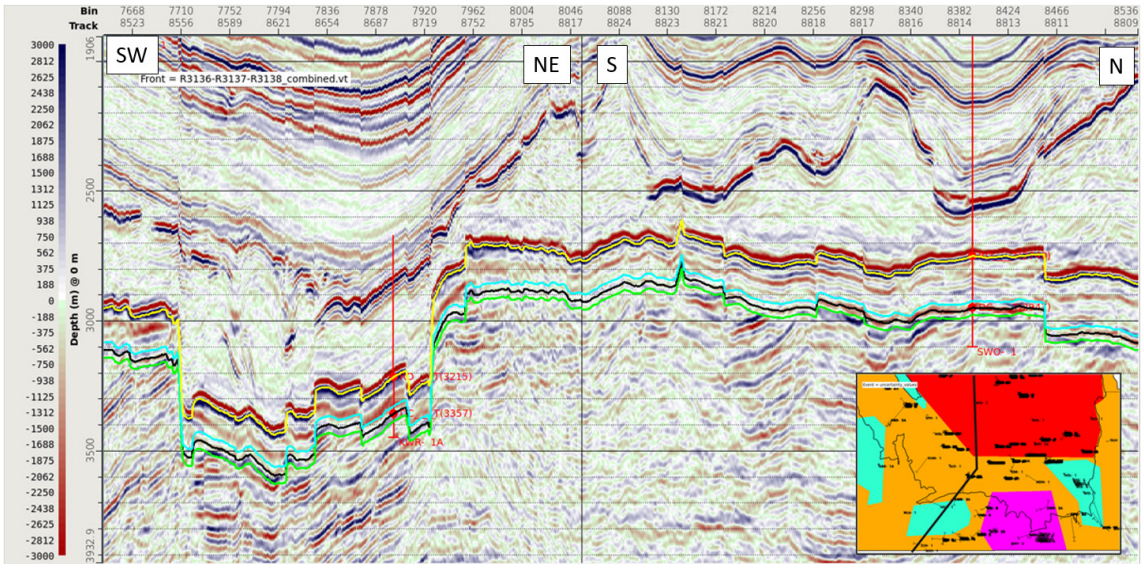

Fig. 27: Seismic cross-section through the southern part of the field and periphery (see inset map). The calculated combined depth uncertainty is added to the base case DC_T depth map (black line), which adds a high case (blue DC_T) and low case (green DC_T) scenario. Depth is in mTVDSS.

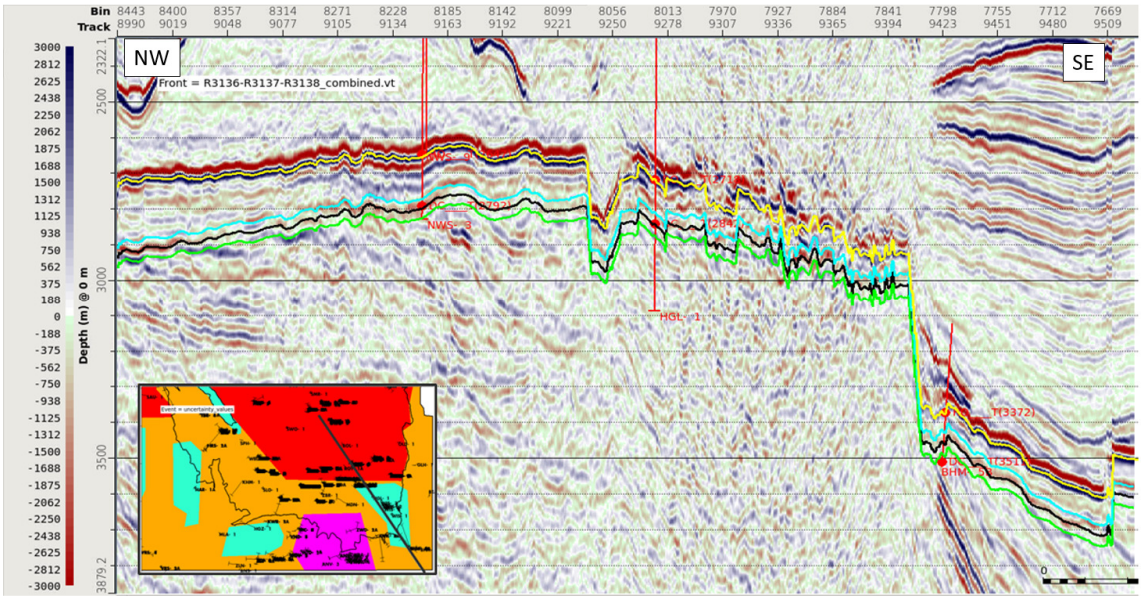

Fig. 28: NW-SE seismic cross-section through the southern part of the field and periphery (see inset map). The calculated combined depth uncertainty is added to the base case DC_T depth map (black line), which adds a high case (blue DC_T) and low case (green DC_T) scenario. Depth is in mTVDSS.

5.5 Step 8: Calculate Carboniferous and Upper Rotliegend bulk rock volume

In this last step, after completing the DC_T seismic interpretation and depth conversion, a rough bulk rock volume is calculated between the gas water contact from the current model and the newly derived top Carboniferous base case depth map. This volume is compared with the bulk rock volume constrained by the LSS_1_B modeled horizon from the current model. The calculations in this section are only a first attempt. Advanced volume calculations are carried out after incorporating the depth surface into the Groningen static model.

The bulk rock volumes are calculated in the 'Volume below surface' tool in the Operations function window in Petrel 2014. The gas-water contact from the present static model is used for the bulk rock volume calculations.

The gas footprint of the new DC_T depth map is 12 km^2 larger than the existing one. This is probably caused by a somewhat shallower DC_T. Besides, a small increase in elevation results in a relatively large increase areally, due to a gentle inclination of the Saalian Unconformity in the central and northern part of the Groningen field. Both Carboniferous gas footprints are combined in figure 29.

The newly derived DC_T constrains a base case Carboniferous bulk rock volume of 31.0 bcm, which is 6.23% (+1.82 bcm) larger than the current model. This implies a decrease of -1.82 bcm bulk rock in the Upper Rotliegend, from 145.2 bcm to 143.4 bcm, which is equal to -1.25% (Table 2).

Obviously, these volume differences are clearly within the same order of magnitude, and they are comparable with volumes from previous studies of 1977 (NAM 6823) and 1989 (NAM 89.2.084). The GWC level has a big impact on the bulk rock volumes, since the 27.2 bcm low case, 33.5 bcm base case and 50.4 bcm high case bulk rock volume of the latter study includes a GWC at -2980m TVDSS, -3000m TVDSS and -3040m TVDSS, respectively.

This attempt indicates that the newly calculated base case Carboniferous bulk rock volume of 31 bcm is close to the average of 29.1 bcm from the current model and 33.5 bcm (ΔV= 2.5 bcm / -7.5%) from the 1989 study, the latter of which is better supported with the new result, rather than 22.1 bcm (ΔV= 8.9 bcm / +40.3%) from the 1977 study.

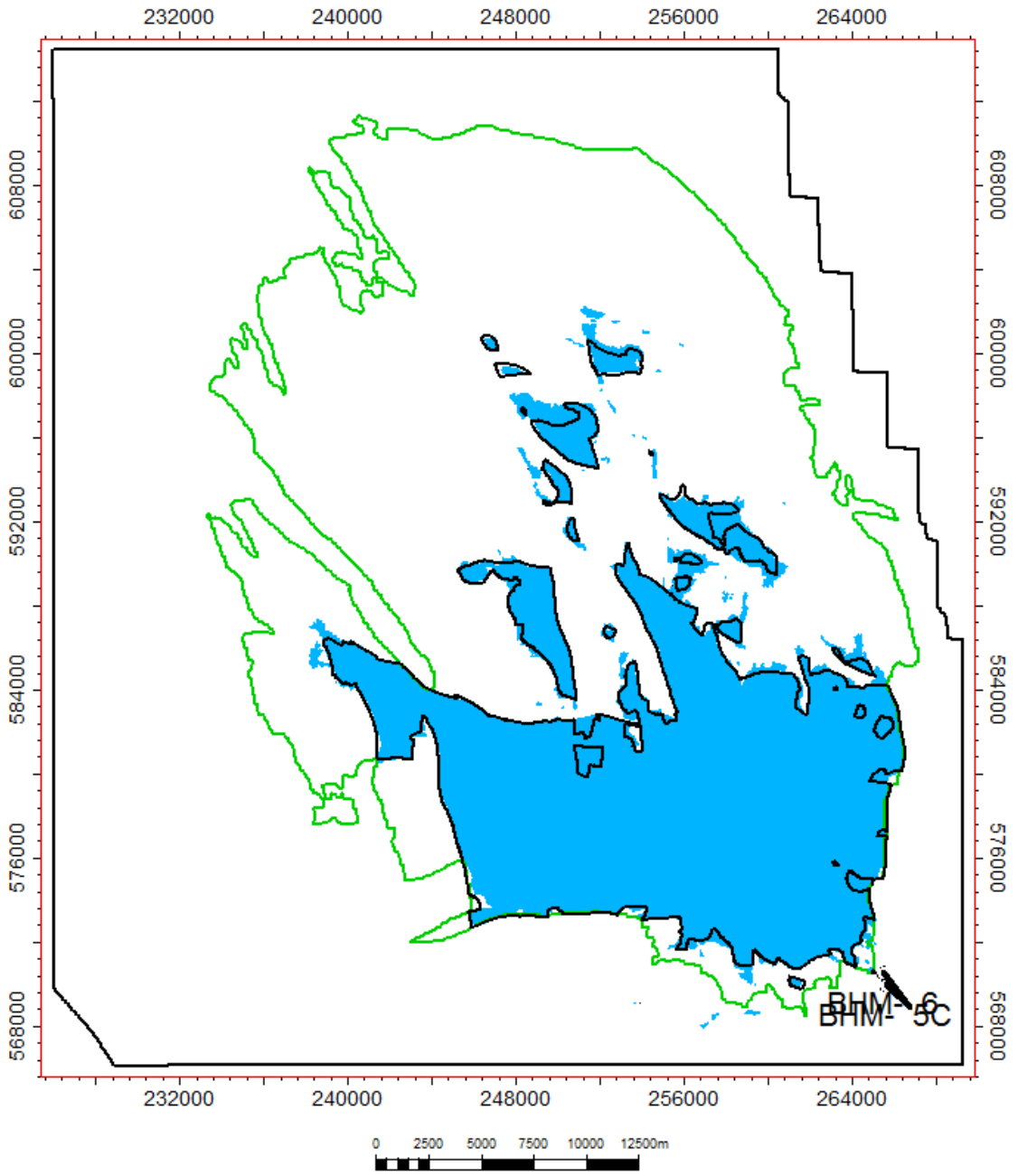

Fig. 29: Comparison between the Carboniferous footprint controlled by the LSS_1_B (black polygon: 296 km^2) and the new DC_T (blue area: 308 km^2). The extra 12 km^2 is mainly accommodated in the central and northern part of the Groningen field (green polygon).

	BULK ROCK VOLUME (bcm)				Area gas footprint (km2)			
	LSS_1_B	DC_T	Δvolume	%	LSS_1_B	DC_T	Δkm^2	%
Carboniferous sequence	29.14	30.96	+1.82	+6.23%	296	308	+12	+4.05%
Slochteren reservoir	145.20	143.39	-1.82	-1.25%				

Table 2: Calculated bulk rock volumes in both the Carboniferous and Upper Rotliegend (Slochteren) reservoir and the area of the two gas footprints, derived from the two different top Carboniferous horizons are compared in this table. The LSS_1_B is the currently used depth horizon and the DC_T is the new horizon. The GWC is kept constant. The calculated volumes in this table are a first attempt and indicates a small to moderate increase of the gas footprint area (+4%) and the GRV (+6%).

6 Conclusions

The main deliverable of this study is a new depth map of the top Carboniferous, which is now available. The following conclusions can be drawn:

Bulk rock volume:

- When comparing the Upper Rotliegend bulk rock volume of the current model (145.2 bcm) with the bulk rock volume constrained by the newly derived base case DC_T depth surface (143.4 bcm), the latter shows a decrease of -1.82 bcm, which is equal to -1.25%. This implies that the bulk rock volume of the gas-bearing part of the Carboniferous section increased with 1.82 bcm, which is equal to a 6.23% increase.

Depth comparison of top Carboniferous:

- For the major part of the Groningen field, the difference between the DC_T and LSS_1_B depth maps is less than 10m. The largest differences occur in the West in the Lauwerszee Trough, where the DC_T is about 50m shallower than the LSS_1_B, and to the northwest, where the DC_T is about 50m deeper than the LSS_1_B.
- The area where the newly defined Carboniferous reaches above the gas-water contact of the Groningen field is 308 km^2 which is 12 km^2 (+4%) larger than the footprint of LSS_1_B depth horizon.

Seismic:

- Seismic data quality at Carboniferous level varies significantly throughout the field. Data quality is negatively impacted by salt pillows and diapirs in the overburden to the South and along the Groningen field periphery. Pull-up effects of this salt can be clearly seen on the DC_T time map. These features are in general present along the southern and western periphery of the field.
- The majority of the DC_T well-tops in the synthetics correspond to a negative amplitude. The central part of the Groningen field shows the largest (negative) amplitudes, which corresponds to the most easily picked area and can be auto-tracked. Lower amplitudes in the southern part of the field are due to poorer seismic data quality, higher fault density and picking of DC_T on zero-crossings in the southern periphery. In these areas, the DC_T reflector is often diffuse and discontinuous, especially in the northern and southern periphery. The reflector is better visible in areas with a clear angular unconformity.
- No flat spots have been recognized on seismic that could point to the presence of the gas water contact in the Carboniferous.

Upper Rotliegend thickness:

- The generated thickness map of the Upper Rotliegend supports the current geological concept of gradual reservoir thickness increase towards the northwest. As an exception to this, the Rotliegend appears to be relatively thin in the elongated, NW-SE oriented graben, in the western periphery of the field. Whether this is due to a mispick, wrong depth conversion or due to a geological reason, like syndepositional faulting, is not well understood.

Upper Rotliegend interval velocities:

- A velocity map of the Upper Rotliegend Group is available. This map is interpolated from average reservoir velocities at 79 well-locations. No obvious lateral velocity trends are found, but there could be subtle correlation between increasing reservoir thickness and decreasing reservoir velocities, which is defined in velocity model 2 in this study.

Well-tie residuals:

- The largest well-tie residuals of 30 m or more are outside the Groningen field or close to its outer limits, i.e. in wells Blijham-5C, Bedum-1, Farmsum-1C, Scheemderzwaag-204C and

Eemskanaal-1. A large positive well-tie residual (+32m) in well Zuidwending-2A is probably due to a mispick in this area of poor seismic data quality.

6.1 Recommendations

- Calculate the Carboniferous bulk rock volume for the high and low case scenarios. Investigate to what extent the Carboniferous gas volume could contribute to gas production and pressure support to the Groningen field. .
- Reservoir properties required for GIIP calculations can be derived with the methods used by Seubring (1994) to define the average petrophysical properties from the Carboniferous well logs and cores.
- Interpret the Carboniferous subgroups on seismic. This should improve our understanding of the internal structural geological setting, the size of Carboniferous fault blocks and eventually identification of (non-)reservoir sequences to improve net-to-gross estimates.

6.2 Additional project Information

Software
All steps in this study, including seismic interpretation, were carried out in Petrel 2014, apart from steps 2, 4, 5 and 7 for which nDI was used. Steps 4 and 5 were later repeated in Petrel 2014 for practicing purposes.

Location
The Top Carboniferous Seismic Interpretation project is stored at the following location:
\\europe.shell.com\tcs\ams\petrel01\epe_land\groningen\nl_groningen\petrel_work\2016_GFR_Bart_DC_T

7 References

- Buggenum, J.M. van, & D.G. Den Hartog Jager, 2007. *Geology of the Netherlands*

  Silesian

- Geluk, M. 2007. *Geology of the Netherlands* – Permian

- NAM report no. 6823, 1977. Groningen field Carboniferous Coal Measures. EP48963.

- NAM report no. 89.2.084, 1989. Volumetric GIIP Carboniferous Groningen Field.

- Rijksgeologische dienst, 2000. Geologische atlas van de diepe ondergrond : blad VI:

  Veendam-Hoogeveen NAM000010590020/1

- Seubring, J., 1994. Petrophysical Evaluation of the Groningen Field Carboniferous. Report No. 26649, BUG no. 397

- V. C. Smith, 1994. Carboniferous Seismic Evaluation Report Groningen Gas Field. NAM rep. No. 27.393, BUG No. 446

- Van Adrichem Boogaert, H.A. & Kouwe, W.F.P., 1993-1997. [Stratigraphic unit]. In: Stratigraphic Nomenclature of the Netherlands.

- Visser, C., Connelly, B., van Dongen, M., Prousa, F., Kelder, O., Van Jaarsveld, J., 2012. Groningen Field Review 2012. Doc. Nr. EP201203204663

- Vrouwe, B., 2007. Structural Analysis of the Groningen High. Master Thesis, NAM/Shell EPE, Faculty of Earth and Life Sciences, Vrije Universiteit Amsterdam, pp. 86.

- Ziegler, P.A., 1990. Geological Atlas of Western and Central Europe (2nd edition),

  Shell Internationale Petroleum Maatschappij, 239 pp.

Appendix

Appendix A: Ten synthetics over the reservoir interval, displayed with sonic log (left) and interval velocity (right). The wells are distributed over the thin and thick reservoir interval within the Groningen field. Intraformational well markers are added to assist further understanding for the time-thickness-based Rotliegend velocity map:

RO_T	→	RO_T (top Rotliegend)
ROSLU_T	→	USS_3.1_T (base Ten Boer / top Upper Slochteren)
ROSLU_B	→	LSS_2.4_T (base Upper Slochteren / Top Ameland Claystone)
ROSLL_T	→	LSS_2.3_T (base Ameland Claystone / top Lower Slochteren)
ROSLL_B	→	LSS_1_B (base Lower Slochteren / base Rotliegend / top Carboniferous)

Well	Study #
BRH-1	26
SDM-1	27
ZRP-1	28
MLA-1	34
TJM-1	49
SDB-1	50
ZBR-1	53
ZWD-1	61
SPI-1	63
NWS-1	65

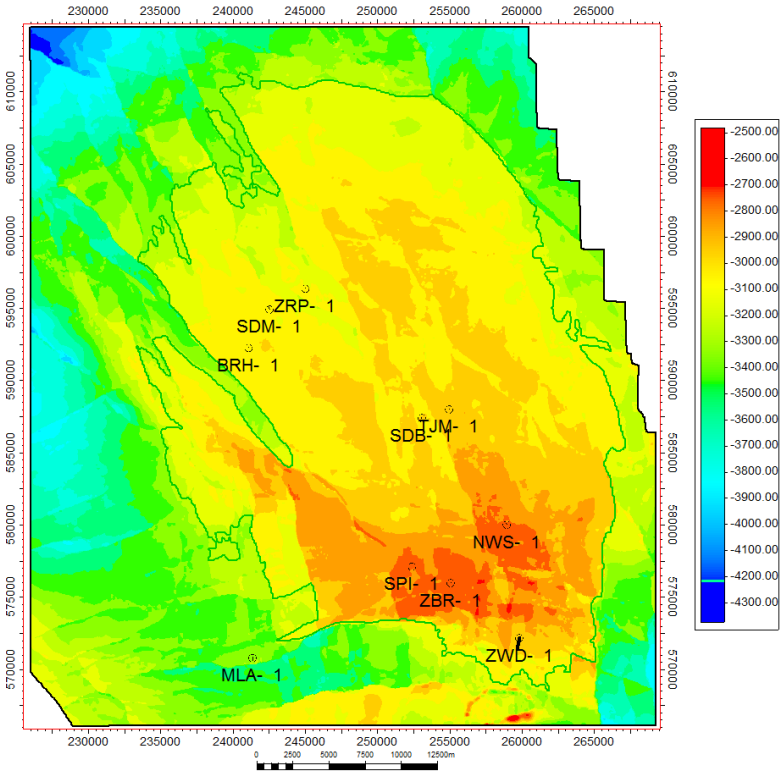

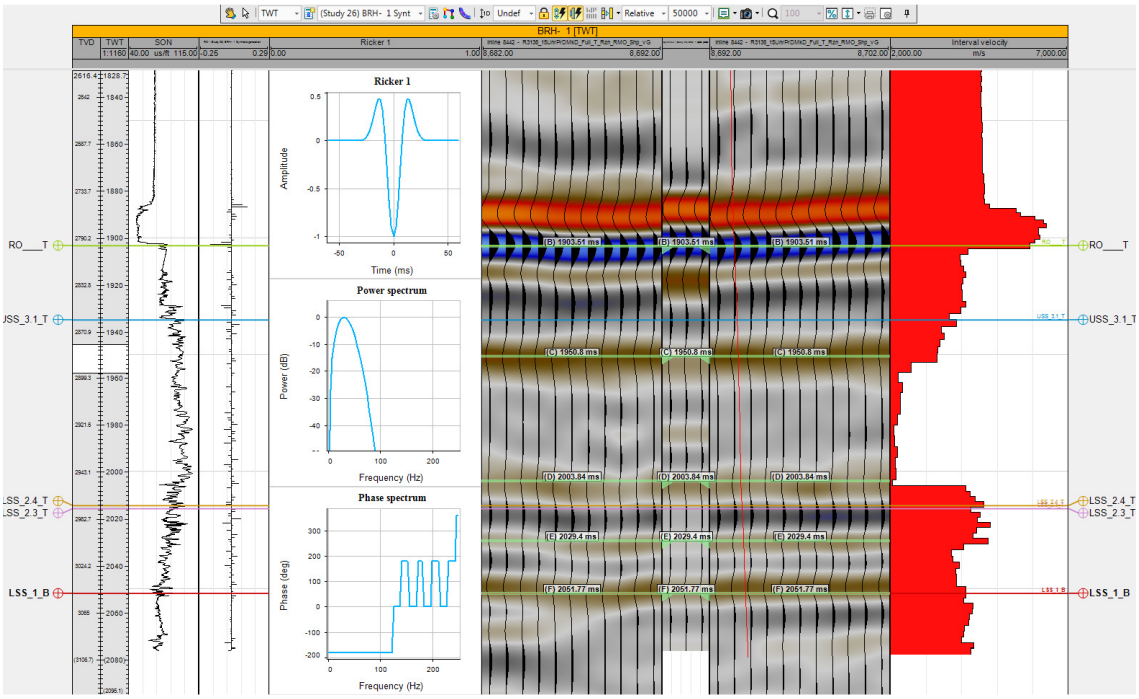
BRH- 1 [TWT]
Ricker 1
Amplitude
Time (ms)
Power spectrum
Power (dB)
Frequency (Hz)
Phase spectrum
Phase (deg)
Frequency (Hz)
RO___T
USS_3.1_T
LSS_2.4_T
LSS_2.3_T
LSS_1_B

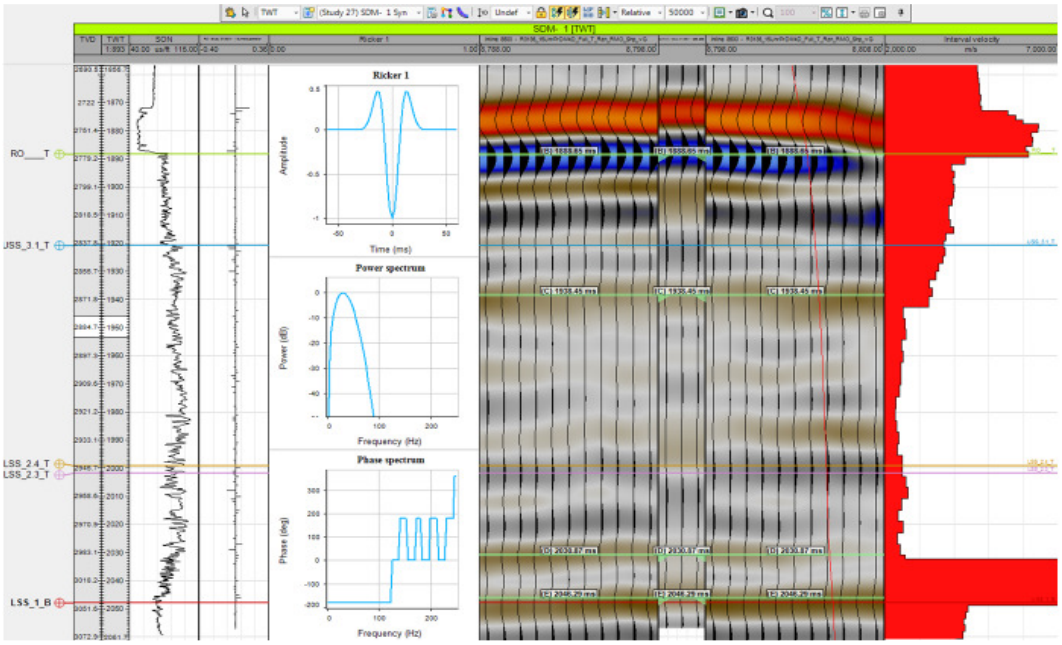
SDM- 1 [TWT]
Ricker 1
Amplitude
Time (ms)
Power spectrum
Power (dB)
Frequency (Hz)
Phase spectrum
Phase (deg)
Frequency (Hz)
RO___T
USS_3.1_T
LSS_2.4_T
LSS_2.3_T
LSS_1_B

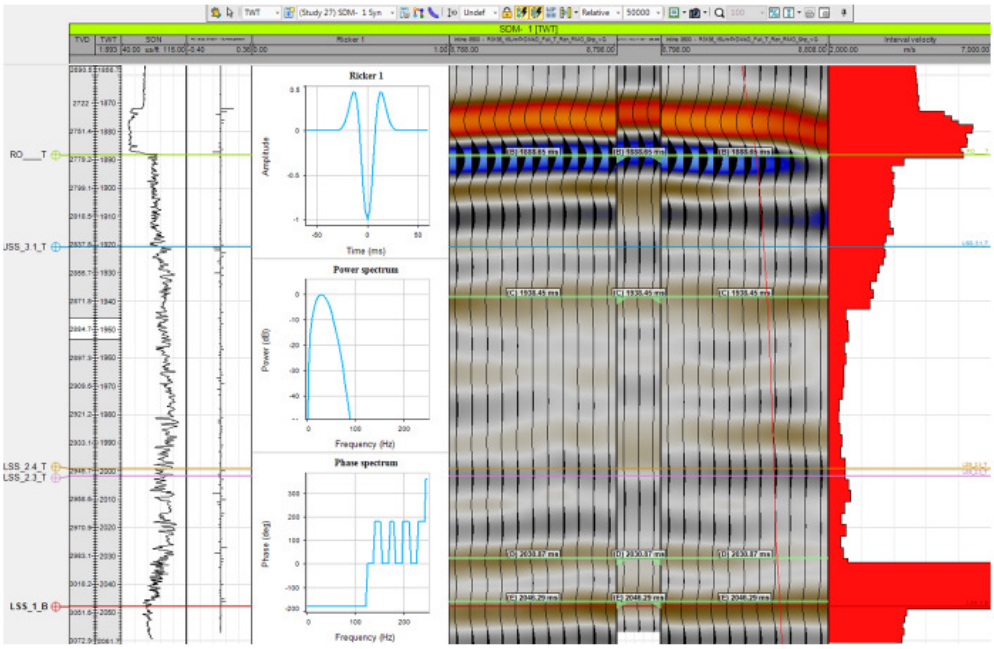
SDM- 1 [TWT]
Ricker 1
Amplitude
Time (ms)
Power spectrum
Power (dB)
Frequency (Hz)
Phase spectrum
Phase (deg)
Frequency (Hz)
RO___T
JSS_3.1_T
LSS_2.4_T
LSS_2.3_T
LSS_1_B

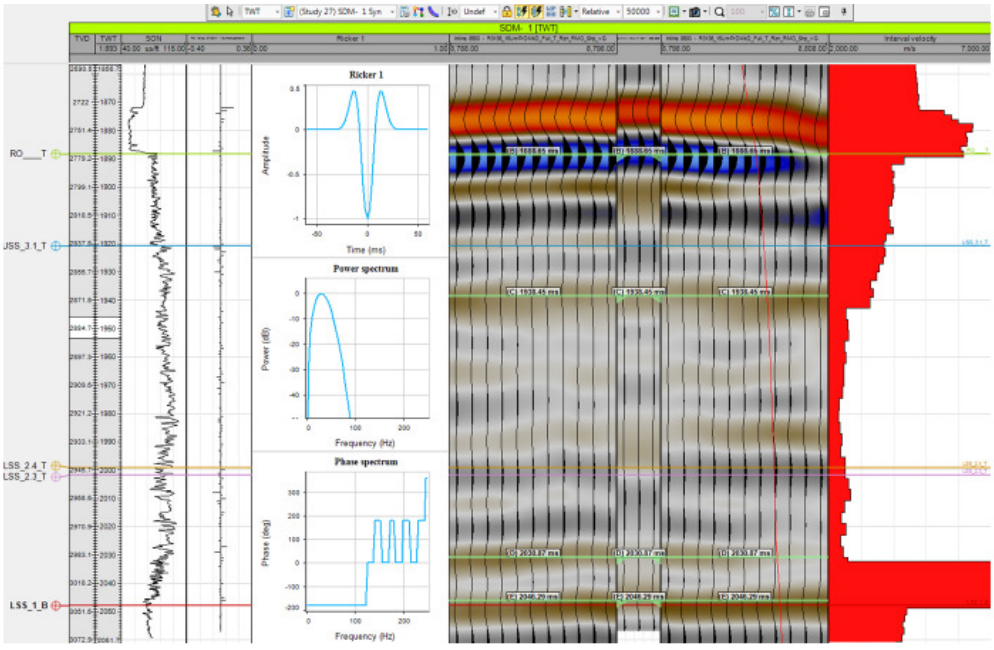
SDM- 1 [TWT]
Ricker 1
Amplitude
Time (ms)
Power spectrum
Power (dB)
Frequency (Hz)
Phase spectrum
Phase (deg)
Frequency (Hz)
RO___T
JSS_3.1_T
LSS_2.4_T
LSS_2.3_T
LSS_1_B

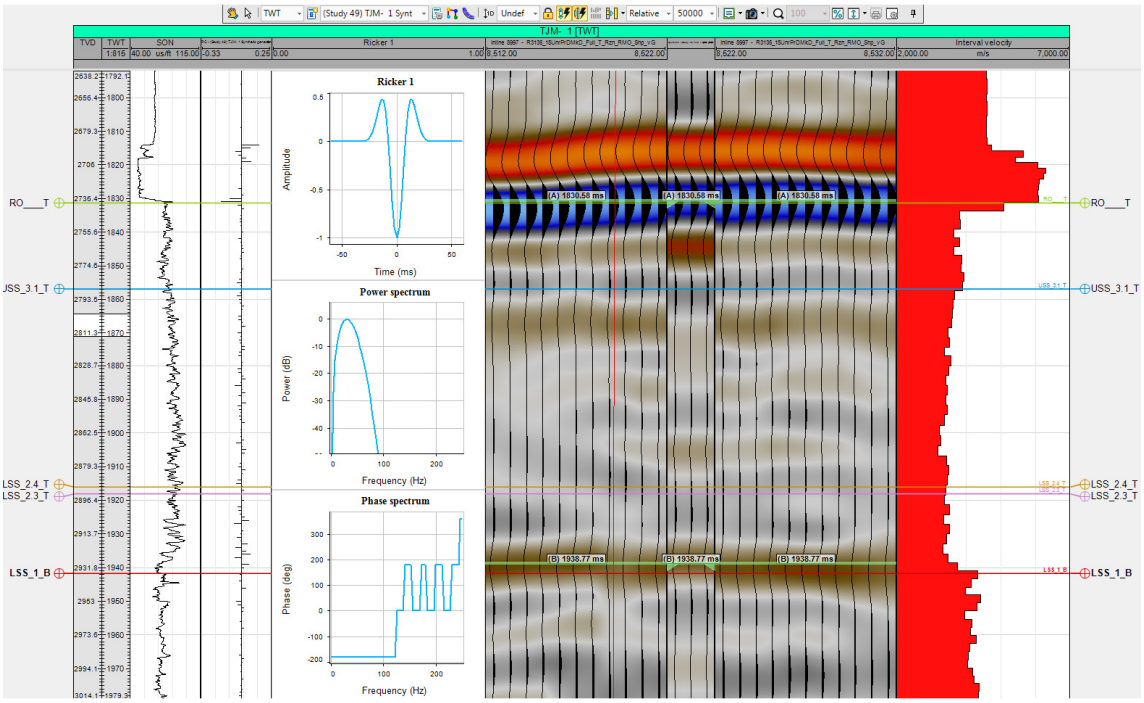
TJM- 1 [TWT]
Ricker 1
Amplitude
Time (ms)
Power spectrum
Power (dB)
Frequency (Hz)
Phase spectrum
Phase (deg)
Frequency (Hz)
RO____T
USS_3.1_T
LSS_2.4_T
LSS_2.3_T
LSS_1_B
(A) 1830.58 ms
(B) 1938.77 ms

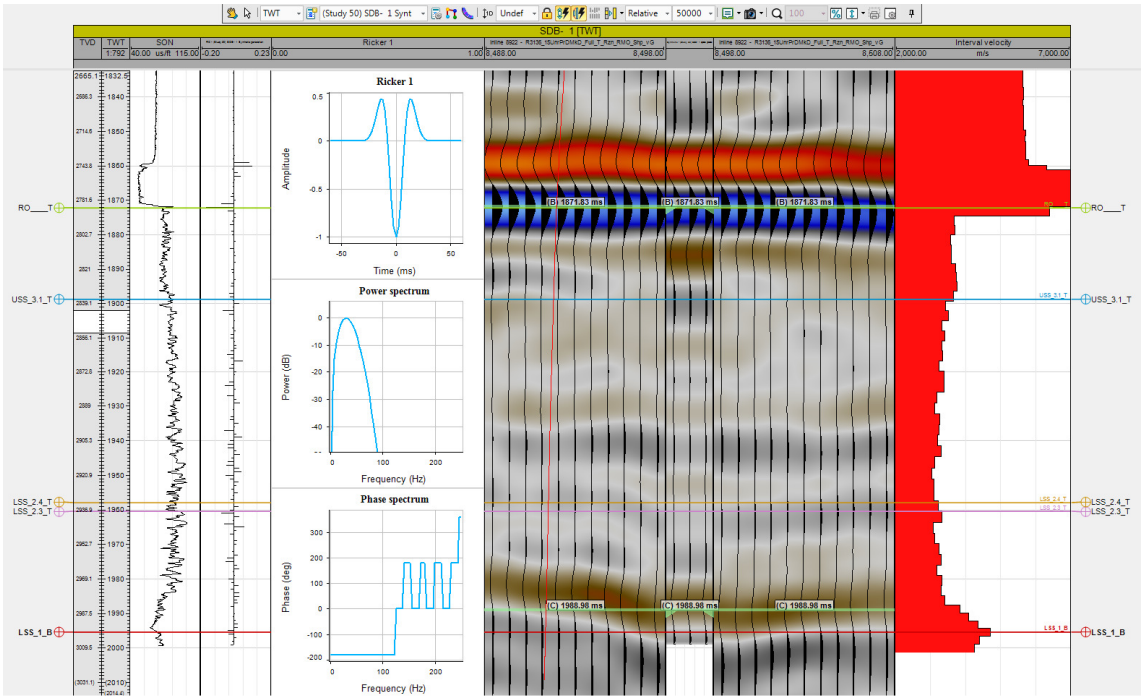
SDB- 1 [TWT]
Ricker 1
Amplitude
Time (ms)
Power spectrum
Power (dB)
Frequency (Hz)
Phase spectrum
Phase (deg)
Frequency (Hz)
RO____T
USS_3.1_T
LSS_2.4_T
LSS_2.3_T
LSS_1_B
(B) 1871.83 ms
(C) 1988.96 ms

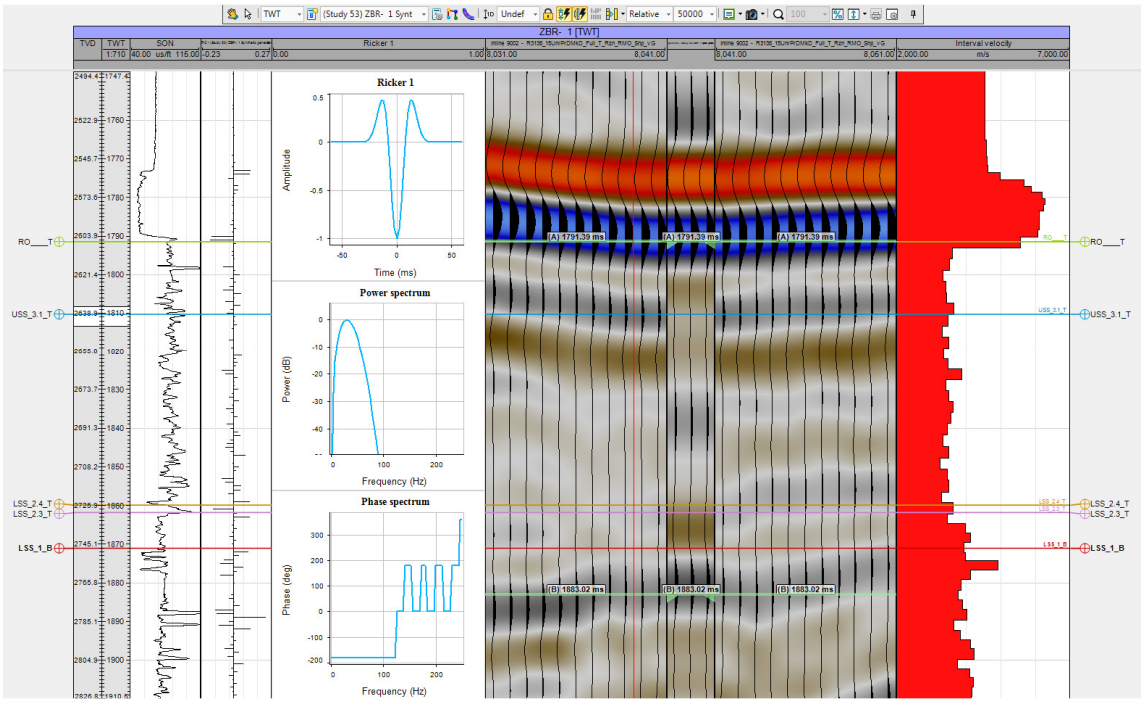
ZBR- 1 [TWT]
Ricker 1
Amplitude
Time (ms)
Power spectrum
Power (dB)
Frequency (Hz)
Phase spectrum
Phase (deg)
Frequency (Hz)
Interval velocity
RO____T
USS_3.1_T
LSS_2.4_T
LSS_2.3_T
LSS_1_B
(A) 1791.39 ms
(B) 1883.02 ms

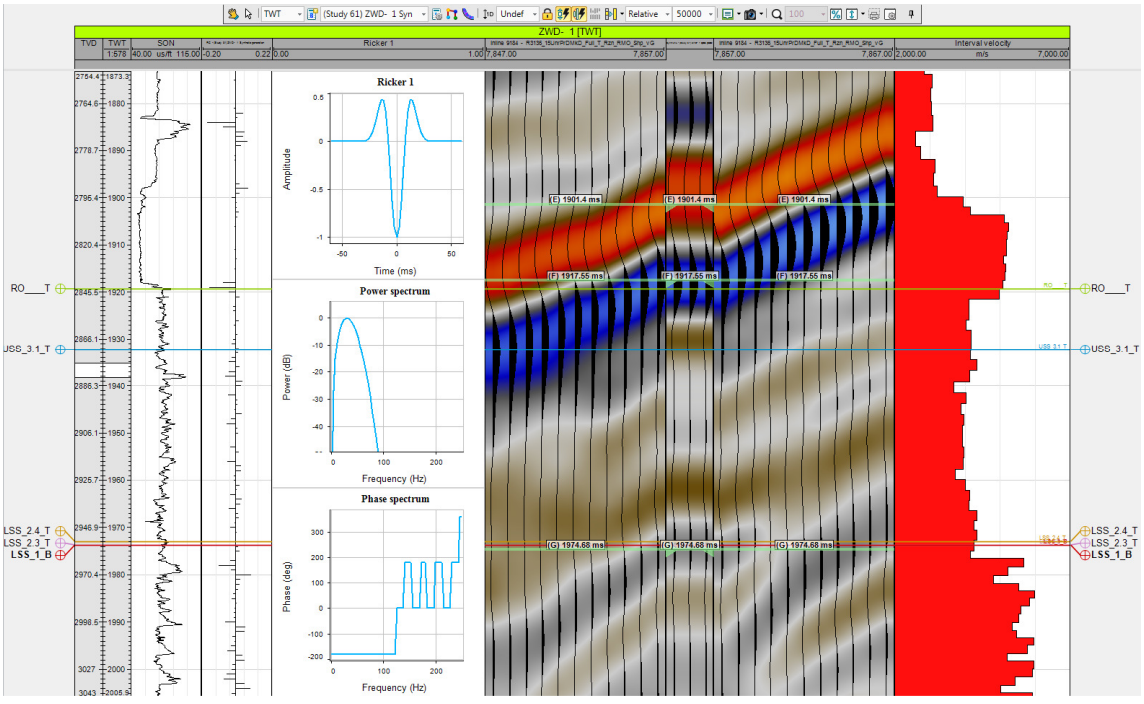
ZWD- 1 [TWT]
Ricker 1
Amplitude
Time (ms)
Power spectrum
Power (dB)
Frequency (Hz)
Phase spectrum
Phase (deg)
Frequency (Hz)
Interval velocity
RO____T
USS_3.1_T
LSS_2.4_T
LSS_2.3_T
LSS_1_B
(E) 1901.4 ms
(F) 1917.55 ms
(G) 1974.68 ms

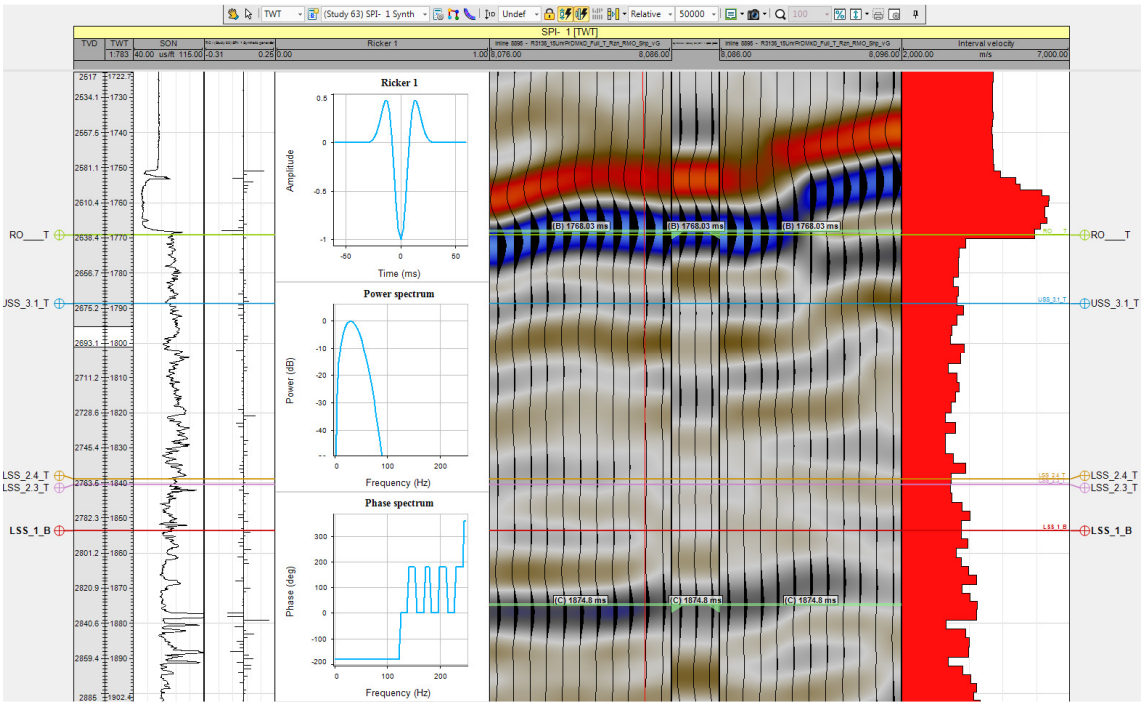

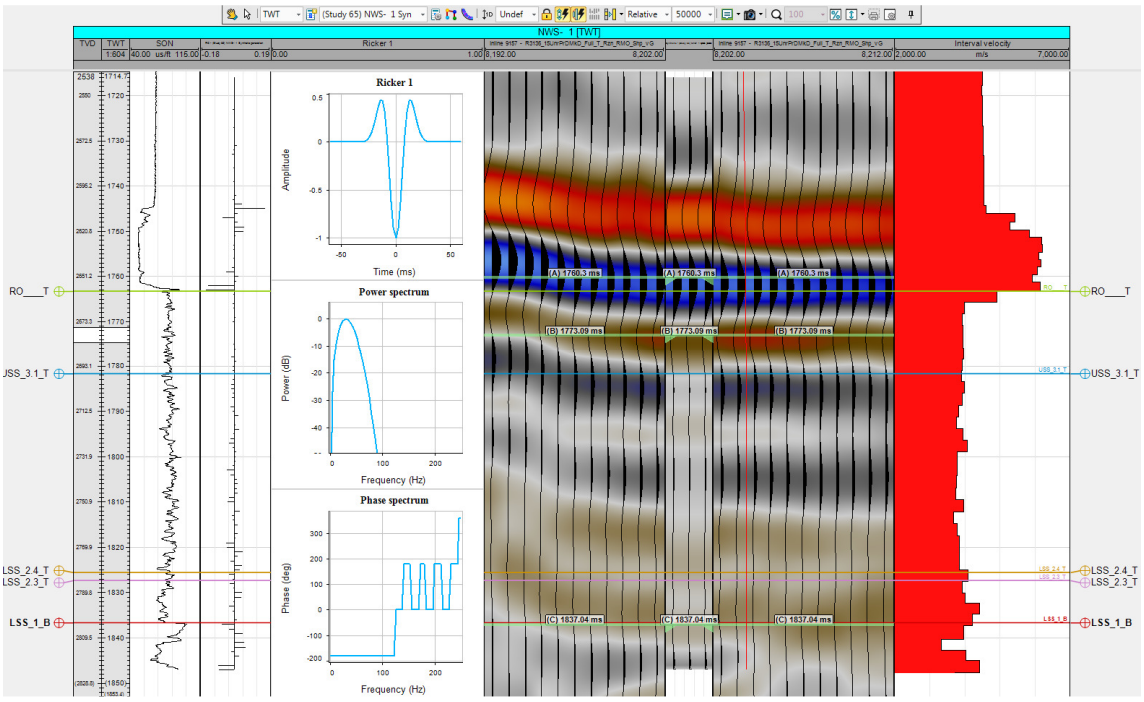

Appendix B: Wells used for well tie-ing DC_T depth horizon. Table is ordered according to decreasing well-tie residual. Faulted wells are left out. Residual values are listed.

Well report for 'Final results/Depth/DC_T_model3_depth.xyz_tied_nofaultedwells' (In Make surface)							
Well	MD	X-value	Y-value	Z-value	Horizon before	Diff before	Horizon after
ZWD- 2A	3520.69	258293.1	570981.2	-3024.57	-3058.07	33.5	-3024.57
EKR- 12	2930.59	259459.4	577849.5	-2771.35	-2787.07	15.72	-2771.35
MWD- 1	2914.22	264302.9	578668	-2893.9	-2906.71	12.81	-2893.9
EMH-Z 1A	3433.46	256256.4	609320.6	-3397.31	-3409.31	12	-3397.31
EKR-210	2803.06	259885.3	577774.5	-2764.62	-2775.54	10.92	-2764.62
EKR-209	2772.66	259890.9	577426.9	-2760.21	-2770.97	10.75	-2760.21

WSM- 1	3374.63	229743.5	595584.8	-3241.83	-3252.5	10.68	-3241.83
SLO- 5	2842.19	246296.9	579143.3	-2832.91	-2842.59	9.68	-2832.91
ZPD- 6	2890.53	261734.2	580772.7	-2866.18	-2874.79	8.61	-2866.18
SDB- 1	3007.39	253084.2	587304.9	-2994.37	-3002.46	8.09	-2994.37
SZW- 1	2841.78	256922.5	577981.6	-2820.17	-2827.96	7.79	-2820.17
SZW- 6	2837.8	257189.6	578034.7	-2822.16	-2829.76	7.6	-2822.16
ZRP- 1	3103.64	245004.5	596485.1	-3093.13	-3100.32	7.19	-3093.13
SAU- 1	3742.38	230510.8	589286.5	-3495.66	-3502.78	7.12	-3495.66
WDV- 2	3214.08	249985.9	567635.7	-2962.87	-2969.98	7.11	-2962.87
SDB- 5	3123.65	253150.9	586886.7	-3003.91	-3010.62	6.71	-3003.91
NWS- 3	2806.21	258759.7	580155.5	-2792.29	-2798.99	6.7	-2792.29
KPD- 12	2986.66	247614.4	580994.7	-2834.48	-2841.15	6.67	-2834.48
EKR-207	2773.48	259933.9	577361.5	-2763.98	-2770.35	6.37	-2763.98
SPI-208	2754.22	252626.1	577093.5	-2742.02	-2748.27	6.25	-2741.83
ZND- 9A	3068.45	248413.7	600674.2	-3005.57	-3011.47	5.91	-3005.57
ZPD- 9	2952.63	262195	580859.9	-2895	-2900.64	5.63	-2895
NWS- 4	2808.51	258836	580199.1	-2795.89	-2801.37	5.48	-2795.49
MWD- 4	2906.54	264182.9	578733.6	-2889.74	-2895.05	5.31	-2889.74
NWS- 2	2810.4	258853.9	580173.1	-2794.85	-2800.14	5.29	-2794.91
AMR- 9	3013.33	256453	591891.5	-2944.65	-2949.45	4.8	-2944.65
SZW- 10	2862.44	256792.2	577894.7	-2820.5	-2825.07	4.56	-2820.5
ZPD- 7	2897.19	261748.6	580843.1	-2874.81	-2879.36	4.55	-2874.81
SZW- 3A	2849.05	257000	578071.7	-2827.62	-2832.15	4.54	-2827.95
SZW- 9	2841.05	256857	578050.3	-2822.16	-2826.55	4.39	-2822.16
SZW- 7	2842.02	257124.2	578025.7	-2826.83	-2830.99	4.16	-2826.84
EKR-208	2827.34	260092.4	577756.6	-2769.25	-2772.94	3.7	-2769.25
MDN- 1	3160.17	257158.6	575393.6	-2753.46	-2756.88	3.42	-2753.46
MDN- 1	3160.17	257158.6	575393.6	-2753.46	-2756.88	3.42	-2753.46
HRS- 1	3316.95	239501.2	581790.2	-3097.55	-3100.96	3.41	-3097.55
AMR- 10	3078.57	256834.7	591781	-2949.9	-2953.23	3.33	-2949.9
AMR- 4	2990.95	256609.2	591621	-2944.59	-2947.91	3.32	-2944.88
ZVN- 6	2911.86	253257.9	579005.1	-2841.56	-2844.83	3.27	-2841.56
ROT- 1A	2772.81	258123.1	579630.1	-2761.72	-2764.99	3.27	-2761.72
SDB- 2	3012.19	253361	587279.2	-3001.56	-3004.74	3.18	-3001.56
SPI-206	2757.26	252572.6	577117.9	-2748.14	-2751.11	2.97	-2748.14
AMR- 8	2968.01	256447.2	591670.2	-2939.8	-2942.72	2.92	-2939.8
NBR- 2	2895.9	254938	579405	-2879.15	-2882.03	2.88	-2879.15
WDV- 5	3074.01	250972.6	568363.5	-3021.63	-3024.46	2.84	-3021.63
SPH- 1	2892.78	244327	583149.1	-2854.59	-2857.43	2.84	-2854.59
EKR-201	2753	259708.8	577256.7	-2740.64	-2743.42	2.79	-2740.64
SPI- 9	2785.94	252059.1	577125.4	-2776.81	-2779.46	2.65	-2776.81
TJM- 6	2931.02	254908.4	588301.7	-2925.65	-2928.25	2.6	-2925.65
EKR- 7	2737.34	259548.4	577216.4	-2719.7	-2722.21	2.51	-2719.7
MWD- 7	2911.92	264298.2	578522.9	-2901.81	-2904.18	2.37	-2901.81
SPI-207	2755.5	252652.4	577155.8	-2745.26	-2747.46	2.21	-2745.62
SAP- 13	2933.26	249671.8	575842.5	-2881.86	-2884.03	2.18	-2881.86
OVS- 8	2992.78	250427.4	590797	-2985.96	-2988.14	2.18	-2985.96
OVS- 8	2992.78	250427.4	590797	-2985.96	-2988.14	2.18	-2985.96
LRM- 2	2989.26	249929.9	596973.2	-2980.44	-2982.57	2.13	-2980.44
POS- 1	2997.36	245698.4	591167.9	-2989.29	-2991.39	2.1	-2989.29
OVS- 1	2995.23	250514.2	590700.4	-2986.45	-2988.54	2.1	-2986.44
NBR- 4A	2898.24	255070.1	579376.9	-2879.67	-2881.71	2.04	-2879.67
SZW-201	2856.01	257246	577974.3	-2825.94	-2827.94	2	-2823.44
BRW- 2A	3114.01	263417.2	590605.5	-3084.13	-3086.05	1.92	-3084.13
AMR- 3	2986.66	256639.9	591627	-2946.85	-2948.68	1.83	-2946.84
OWG- 2	2920.17	256112.3	586073.9	-2910	-2911.8	1.81	-2910
ZND- 2	3051.24	247839.3	600848.2	-3004.56	-3006.34	1.78	-3004.56
AMR- 11	2956.84	256498.2	591678.7	-2944.04	-2945.81	1.77	-2943.96
SLO- 3	2844.13	246179.4	579276.7	-2833.3	-2834.98	1.68	-2833.3
OPK- 2A	3767.01	263881.1	569010.8	-3045.51	-3047.1	1.59	-3045.51
KHM- 1	4034.35	242972.9	575891.2	-3080.19	-3081.64	1.45	-3080.19
TJM- 10	2934.15	254977.2	588190.4	-2924.79	-2926.14	1.35	-2924.79
AMR- 2	2979.89	256650.8	591637	-2947.94	-2949.29	1.34	-2947.94
EKR- 11	2849.7	259213.2	577029.1	-2819.6	-2820.9	1.3	-2819.6
ROD-201A	3390.76	226873.8	571330.7	-3150.19	-3151.46	1.27	-3150.19
TJM- 4	2936.31	254910.2	588092.8	-2927.44	-2928.6	1.15	-2928.53
MWD- 8	2912.87	264325.1	578554.1	-2904.07	-2905.22	1.15	-2903.62
SPI- 4	2792.55	252113	577197.8	-2779.18	-2780.27	1.09	-2779.18

ANV- 1	3128.13	257404.4	568074.6	-3115.06	-3116.15	1.09	-3115.06
ZND- 1	3006.14	248047.1	600486.5	-2997.56	-2998.62	1.06	-2997.56
OVS- 3	2994.71	250479.9	590895	-2985.69	-2986.73	1.04	-2985.69
MLA- 1	3339.42	241395.1	570686.5	-3306.45	-3307.36	0.91	-3306.45
DZL- 1	3033.23	260653.7	591995.6	-3027.72	-3028.54	0.81	-3027.73
SPI-209	2755.31	252696.8	577116.3	-2746.53	-2747.24	0.71	-2746.42
SPI- 2	2791.59	252319.2	577147.2	-2782.09	-2782.77	0.68	-2782.02
SCB- 1	2983.92	257639.7	588386.5	-2976.86	-2977.52	0.67	-2976.86
BOL- 1	2853.85	257713.4	582605.8	-2845.15	-2845.81	0.66	-2845.15
MOW-Z 1	3421.11	249105.7	614497.2	-3377.14	-3377.75	0.61	-3377.14
SAP- 1	2899.48	249548.7	575593.3	-2885.9	-2886.51	0.6	-2885.9
SPI- 10	2786.7	252075.5	577186.8	-2777.88	-2778.45	0.57	-2777.86
SCB- 5	2984.15	257323.1	588339	-2977.5	-2978.06	0.56	-2977.5
AMR- 6	3077.11	256321.9	591931.9	-2943.58	-2944.14	0.55	-2943.58
OPK- 4A	3472.1	261354.4	569938.8	-3001.4	-3001.94	0.54	-3001.4
GLH- 1	3199.26	267397.5	579797.3	-3128.91	-3129.44	0.52	-3128.91
VRS- 2	3202.32	233606.3	566334.5	-3189.37	-3189.86	0.49	-3189.37
ZVN- 9	2839.3	253179.3	579338.4	-2829.54	-2829.82	0.28	-2829.54
NBR- 6A	2900.06	255450.3	579360.2	-2855.28	-2855.55	0.27	-2855.28
UHZ- 1	3103.82	242627.3	605824.2	-3095.32	-3095.55	0.23	-3095.32
USQ- 1	3210.34	237058.8	604912	-3194.96	-3195.17	0.21	-3194.96
SAP- 8	2901.12	249388.2	575615.4	-2880.99	-2880.91	-0.09	-2880.99
ZPD- 8	2926.59	262022.8	581093.7	-2902.49	-2902.37	-0.12	-2902.49
SCB- 10	2983.41	257564.9	588426.4	-2977.96	-2977.79	-0.17	-2977.96
BRW- 3	3125.53	263395.1	590262.2	-3078.17	-3077.97	-0.2	-3078.17
OWG- 10	2920.34	256035.5	585968.7	-2905.92	-2905.7	-0.22	-2905.92
TJM- 1	2936.84	254905.6	588006.8	-2930.04	-2929.71	-0.33	-2930.04
HND- 1	3138.08	256867.9	602469.5	-3126.63	-3126.13	-0.51	-3126.63
BHM- 2	3652.41	267449.6	568418.2	-3495.47	-3494.96	-0.52	-3495.47
TJM- 7	2934.52	254927.9	588371.1	-2926.78	-2926.26	-0.52	-2926.78
ANV- 3	3165.36	255202.2	566544.6	-3103.32	-3102.8	-0.53	-3103.32
ROD-101	3143.26	226077.7	572697.5	-3134.98	-3134.44	-0.54	-3134.98
NBR- 8	2907.02	254746.5	579434	-2870.39	-2869.81	-0.58	-2870.39
BRH- 1	3050.7	240996.3	592366.8	-3040.41	-3039.81	-0.6	-3040.41
KPD- 4	2872.81	246566.1	580891	-2862.09	-2861.43	-0.65	-2862.09
TJM- 9	2934.03	254971.3	588305.3	-2926.48	-2925.83	-0.65	-2926.51
NWS- 1	2808.96	258830.2	580113	-2797.23	-2796.51	-0.72	-2797.23
SDM- 1	3072.67	242420	595158.6	-3040.05	-3039.18	-0.88	-3040.05
SWO- 1	2953.97	250375.3	584838	-2947.68	-2946.79	-0.89	-2947.68
AMR- 12A	3317.5	255821.3	592792.2	-2951.68	-2950.79	-0.9	-2951.68
TJM- 3	2935.27	254919.9	588069.2	-2929.13	-2928.19	-0.93	-2928.97
UTB- 2	2766.65	255252.8	577489.5	-2758.01	-2757.05	-0.97	-2758.01
OWG- 4	2924.89	256124.7	585979.4	-2909.65	-2908.65	-1	-2909.65
SCB- 9	2983.73	257478.6	588450.5	-2977.45	-2976.4	-1.05	-2977.45
EKR-202	2757.03	259789.5	577263.5	-2744.32	-2743.25	-1.07	-2745.06
NWS- 7	2807.31	258969.4	580183.6	-2798.13	-2797.03	-1.11	-2798.14
UTB- 7	2766.91	255239.5	577429.6	-2757.34	-2756.15	-1.19	-2757.34
HAR- 1A	3359.35	238117.2	576835	-3351.01	-3349.82	-1.19	-3351.01
TJM- 5	2938.69	254886.6	588182.1	-2930.98	-2929.78	-1.2	-2930.97
BRW- 4	3150.17	263427.5	590938.5	-3092.71	-3091.33	-1.38	-3092.71
BRW- 2	3099.18	263513.6	590530.7	-3084.01	-3082.59	-1.42	-3084.01
TJM- 11	2936.08	254986.6	588127.5	-2926.55	-2925.07	-1.48	-2926.66
UHM- 1A	3166.88	249378	607952.6	-3154.3	-3152.81	-1.49	-3154.3
KWR- 1A	3422.96	247473.5	572346.8	-3356.76	-3354.9	-1.85	-3356.76
ZWD- 1	3117.14	259784.1	572163.6	-2946.37	-2944.49	-1.88	-2946.37
SZW- 2	2848.64	256943.5	578062	-2829.49	-2827.58	-1.91	-2829.49
SPI- 1	2790.24	252377.4	577146.7	-2782.32	-2780.41	-1.91	-2782.32
RDW- 1	3361.21	233980.1	596175.5	-3328.84	-3326.92	-1.91	-3328.84
SSM- 2	4239.78	226026.2	592972	-3759.7	-3757.7	-2	-3759.7
PAU- 1	3371.83	247168.8	588939.6	-2993.88	-2991.81	-2.08	-2993.89
KPD- 11	2850.7	246723.1	581150.2	-2813.89	-2811.8	-2.09	-2813.89
KPD- 5	2872.59	246482.9	580927	-2860.35	-2858.18	-2.16	-2860.49
SZW-203	2860.69	257186.8	577984.9	-2826.1	-2823.92	-2.17	-2823.32
TJM- 8	2934.69	254980	588358.8	-2926.6	-2924.41	-2.2	-2926.46
LRM- 7	2995.02	250279.7	597031.9	-2986.27	-2984.05	-2.22	-2986.27
HGL- 1	2853.93	261820.1	575600.9	-2841.48	-2839.26	-2.23	-2841.48
GHS-Z 5	3384.24	263674.7	601871.5	-3382.65	-3380.39	-2.26	-3382.64
ZVN- 4	2853.48	253145.5	579262.1	-2843.59	-2841.12	-2.47	-2843.59

SPI- 8	2797.34	252342.4	577169.2	-2784.97	-2782.38	-2.59	-2784.12
SAP- 9	2898	249363	575553.8	-2881.57	-2878.88	-2.7	-2881.55
ZVN- 3A	2885.59	253370.3	579005.2	-2848.32	-2845.55	-2.77	-2848.32
POS- 4	3002.26	245600.3	591345.6	-2994.49	-2991.69	-2.8	-2994.49
NBR- 7	2895.11	255005.9	579446.2	-2875.75	-2872.88	-2.87	-2876.37
SZW-202	2852.02	257252	577971.3	-2830.27	-2827.29	-2.97	-2822.35
WBL- 1	2881.16	245158	580861.2	-2868.2	-2865.06	-3.14	-2868.2
HGZ- 1	3736.39	244218.3	572357.5	-3068.6	-3065.38	-3.22	-3068.6
ZPD- 1	2914.49	261935.1	580576.6	-2899.68	-2896.45	-3.23	-2899.68
ZVN- 10	2844.38	253236.9	579332.8	-2835.03	-2831.79	-3.24	-2834.9
EKR-205	2872.8	259518.7	577078.2	-2830.31	-2826.91	-3.4	-2830.31
PAU- 3	3027.6	245888.2	588355	-3015.19	-3011.79	-3.41	-3015.24
OWG- 11	2928.92	256048.6	586056.1	-2912.44	-2908.91	-3.53	-2912.41
TJM- 2B	2985.12	255322.9	588106.7	-2923.82	-2920.27	-3.55	-2923.82
SDB- 11	3041.57	253563	587574.4	-3018.02	-3014.36	-3.66	-3018.02
SLO- 6C	2859.85	246303.5	579437.1	-2837.93	-2834.24	-3.7	-2837.93
OVS- 10	2994.46	250409.6	590939.2	-2987.96	-2984.25	-3.71	-2987.96
ZBR- 1	2747.73	255048.6	576012	-2740.56	-2736.77	-3.79	-2740.56
POS- 9	3001.56	245725.3	591242	-2992.53	-2988.67	-3.87	-2992.53
NBR- 3A	2891.73	255033.4	579442.8	-2876.72	-2872.85	-3.87	-2876.72
BHM- 4	3693.56	267508	568909.1	-3472.1	-3468.17	-3.93	-3472.1
UTB- 9	2779	255446.9	577471.6	-2765.61	-2761.59	-4.02	-2765.61
NWS- 5	2811.18	258932.4	580253.3	-2800.29	-2796.23	-4.06	-2800.29
BIR- 2A	3117.79	254942.3	600160.2	-3029.9	-3025.83	-4.07	-3029.9
SPI-204	2767.88	252495	577178.5	-2758.41	-2754.31	-4.1	-2759.83
ODP- 1	3270.13	239227.9	601693.7	-3128.08	-3123.92	-4.16	-3128.08
NWS- 9	2803.23	258760.8	580035.4	-2790.77	-2786.55	-4.22	-2790.77
UTB- 8	2768.88	255196.1	577465.9	-2758.5	-2754.12	-4.38	-2758.35
FRB- 8	2879.32	247962.5	578922.6	-2864.79	-2860.34	-4.46	-2864.79
SPI-202	2789.94	252418.3	577124.4	-2780.53	-2775.79	-4.74	-2781.64
KPD- 6	2873.72	246427.5	580940.9	-2861.31	-2856.55	-4.76	-2861.31
ZPD- 11	2929.66	262075.8	580690.2	-2893.64	-2888.85	-4.79	-2893.66
SZW- 4	2846.67	257132.9	578101.4	-2831.23	-2826.22	-5.01	-2831.22
SLO- 9	2847.37	246425.1	579119.9	-2832.47	-2827.39	-5.08	-2832.47
ZPD- 10	2925.82	262013.9	580706.5	-2895.78	-2890.65	-5.13	-2895.78
ZVN- 13	2888.24	253475.4	579080.3	-2852.7	-2847.34	-5.36	-2852.7
NBR- 5	2891.51	255032	579471.6	-2875.47	-2869.98	-5.49	-2875.83
ZPD- 2	2912.38	261941.2	580673.7	-2900.57	-2894.77	-5.8	-2900.57
PAU- 2	3029.24	245830.7	588306.2	-3018.1	-3011.9	-6.2	-3018.1
UTB- 1B	2903.35	254838.2	578024.8	-2793.03	-2786.46	-6.57	-2793.03
LRM- 1	3080.88	249626.8	596505.6	-2969.91	-2963.25	-6.66	-2969.91
ZND- 11B	3080.52	248297.5	600087.9	-2990.64	-2983.92	-6.72	-2990.64
BRW- 5	3193.74	263884	591177.1	-3082.92	-3075.8	-7.12	-3082.92
FRB- 6	2875.87	248123.6	578936.2	-2863.88	-2856.75	-7.13	-2863.88
SPI-201	2794.48	252435.5	577105.2	-2780.91	-2773.59	-7.32	-2780.91
AMR- 7	3063.74	256207.5	591976.7	-2941.44	-2933.85	-7.59	-2941.44
NWS- 6	2809.07	259009.3	580283.8	-2800.01	-2792.32	-7.7	-2800.02
NWS- 8	2817.15	259018.5	580275.1	-2800.34	-2792.27	-8.07	-2799.88
WDV- 3	3157.64	251189.9	568073.9	-3041.84	-3033.63	-8.21	-3041.84
WDV- 4	3092.92	250846.9	567831.6	-3057.05	-3048.69	-8.36	-3057.05
FRB- 4	2869.41	248118.5	578859.4	-2860.82	-2852	-8.82	-2860.88
ZVN- 11	2857.06	253306.6	579353.2	-2847.3	-2838.25	-9.06	-2847.3
FRB- 3	2870.38	248147.6	578846.9	-2859.07	-2849.73	-9.34	-2859.07
FRB- 7	2876.46	248084	578937.7	-2865.61	-2856.22	-9.39	-2865.16
SAP- 14	2910.17	249634.5	575667.7	-2889.1	-2879.69	-9.41	-2889.1
NBR- 9	2872.86	255210.6	579545.7	-2863.76	-2854.35	-9.41	-2863.76
MWD- 9A	2905.42	264060.8	578531.8	-2896.1	-2886.68	-9.43	-2896.1
FRB- 5	2871.77	248087	578842.9	-2861.92	-2852.5	-9.43	-2861.77
FRB- 2	2869.08	248236.8	578858.7	-2858.52	-2847.33	-11.19	-2858.73
EKR-206	2769.52	259835	577275.1	-2756.79	-2745.17	-11.62	-2756.79
SPI-203	2788.94	252445.4	577161.2	-2778.85	-2766.02	-12.83	-2782.15
GHS-Z 3	3462.97	263758	603533.4	-3459	-3445.51	-13.49	-3459
SZW-208	2868.92	257427	577949.8	-2841.68	-2828.17	-13.51	-2841.68
BIR- 3	3035.16	254822.7	599777.4	-3019.15	-3005.29	-13.85	-3019.15
PPS-Z 1	3431.27	259374.7	598914.4	-3082.01	-3067.87	-14.14	-3082.01
SLO- 4	2856.65	246089.8	579136.6	-2834.9	-2820.32	-14.58	-2834.9
FRB- 1	2871.96	248234.5	578922.5	-2862.46	-2847.14	-15.32	-2862.46
SDB- 7	3175.22	252910.7	586940	-3027.87	-3011.98	-15.89	-3027.87

OPK- 3A	5174.27	263100.6	567055.3	-3319.41	-3302.98	-16.43	-3319.41
SZW-210	2871.75	257474.6	577956.2	-2842.3	-2825.39	-16.91	-2842.44
EKR-203	2756.66	259849	577187.9	-2743.4	-2725.96	-17.43	-2743.41
EKL- 11	2924.94	241333	584667.6	-2893.39	-2875.6	-17.79	-2893.39
EKL- 7	2948.87	241323.4	584129.1	-2879.44	-2861.35	-18.09	-2879.44
EKR-204	2949.76	259638.9	576877	-2864.27	-2846.11	-18.16	-2864.27
EKL- 9	2922.9	241391.5	584371.1	-2891.02	-2872.84	-18.18	-2891.02
MWD- 3	2909.56	264063.2	578655.3	-2899.52	-2881.05	-18.47	-2899.52
BHM- 3	3593.05	266566	568993	-3558.79	-3539.35	-19.44	-3558.79
EKL- 10	2924.17	241344.6	584526.7	-2892.71	-2872.26	-20.44	-2892.71
BHM- 6	4216.55	265489.2	570590.7	-3472.93	-3452.48	-20.45	-3472.93
BDM- 1	3295.22	233242.8	590298.9	-3128.9	-3107.61	-21.29	-3128.9
FRM- 1C	4147.72	258258.2	596756	-3045.11	-3020.4	-24.71	-3045.11
EKL- 4	3065.36	242437.2	584626.1	-2881.22	-2855.34	-25.88	-2881.22
SZW-209	2846.6	257555.7	578093.1	-2832.16	-2803.11	-29.05	-2832.19
SZW-204C	2850.08	257503.6	578111.1	-2825.2	-2794.19	-31	-2825.2
BHM- 5C	3913.83	265611.1	569987.9	-3496.28	-3464.07	-32.21	-3496.28
VLV- 1	3848.48	273708.6	565517	-3693.07	Outside		Outside
NSS- 1A	3981.63	275169.5	577714.7	-3930.22	Outside		Outside
LNB- 1	3922.91	270341.1	569864.8	-3800.43	Outside		Outside
GHS-Z 4	3500.25	263778	604820.7	-3494.54	Outside		Outside
ETV- 1B	3219.96	249340.7	564317.6	-3073.41	Outside		Outside
BTA- 1	3491.14	269320.9	575739.2	-3275.69	Outside		Outside